Chaos and chaos detection techniques

Haris Skokos

Department of Mathematics and Applied Mathematics
University of Cape Town
Cape Town, South Africa

E-mail: haris.skokos@uct.ac.za
URL: http://math_research.uct.ac.za/~hskokos/

Outline

- Dynamical Systems - Chaos
  - ✓ Hamiltonian models – Variational equations
  - ✓ Symplectic maps – Tangent map
  - ✓ Chaos: Sensitive dependence on initial conditions
- Brief description of chaos detection methods
- Chaos Indicators
  - ✓ Lyapunov exponents
  - ✓ Smaller ALignment Index – SALI
    - Definition
    - Behavior for chaotic and regular motion
    - Applications
  - ✓ Generalized ALignment Index – GALI
    - Definition - Relation to SALI
    - Behavior for chaotic and regular motion
    - Application to time-dependent models

Autonomous Hamiltonian systems

Consider an N degree of freedom autonomous Hamiltonian system having a Hamiltonian function of the form:

$$H(\overbrace{q_1,q_2,\ldots,q_N}^{\text{positions}},\ \overbrace{p_1,p_2,\ldots,p_N}^{\text{momenta}})$$

Autonomous Hamiltonian systems

Consider an N degree of freedom autonomous Hamiltonian system having a Hamiltonian function of the form:

$$H(\underbrace{q_1,q_2,\ldots,q_N}_{\text{positions}},\ \underbrace{p_1,p_2,\ldots,p_N}_{\text{momenta}})$$

The time evolution of an orbit (trajectory) with initial condition

$$P(0)=(q_1(0),\ q_2(0),\ldots,q_N(0),\ p_1(0),\ p_2(0),\ldots,p_N(0))$$

is governed by the Hamilton's equations of motion

$$\frac{dp_i}{dt} = -\frac{\partial H}{\partial q_i}\ ,\qquad \frac{dq_i}{dt} = \frac{\partial H}{\partial p_i}$$

Autonomous Hamiltonian systems

Consider an N degree of freedom autonomous Hamiltonian system having a Hamiltonian function of the form:

$$H(\underbrace{q_1,q_2,\ldots,q_N}_{\text{positions}}, \underbrace{p_1,p_2,\ldots,p_N}_{\text{momenta}})$$

The time evolution of an orbit (trajectory) with initial condition

$$P(0)=(q_1(0), q_2(0),\ldots,q_N(0), p_1(0), p_2(0),\ldots,p_N(0))$$

is governed by the Hamilton's equations of motion

$$\frac{dp_i}{dt} = -\frac{\partial H}{\partial q_i} \quad , \quad \frac{dq_i}{dt} = \frac{\partial H}{\partial p_i}$$

Phase space: the 2N dimensional space defined by variables $q_1,q_2,\ldots,q_N, p_1,p_2,\ldots,p_N$

Symplectic Maps

Consider an 2N-dimensional symplectic map T. In this case we have discrete time.

The evolution of an orbit with initial condition

$$P(0)=(x_1(0), x_2(0),\ldots,x_{2N}(0))$$

is governed by the equations of map T

$$P(i+1)=T\,P(i)\ ,\ \ i=0,1,2,\ldots$$

Example (Hénon-Heiles system)

Example (Hénon-Heiles system)

$$H = \frac{1}{2}\left(p_x^2 + p_y^2\right) + \frac{1}{2}\left(x^2 + y^2\right) + x^2 y - \frac{1}{3}y^3$$

Example (Hénon-Heiles system)

$$H = \frac{1}{2}\left(p_x^2 + p_y^2\right) + \frac{1}{2}\left(x^2 + y^2\right) + x^2 y - \frac{1}{3}y^3$$

THE ASTRONOMICAL JOURNAL VOLUME 69, NUMBER 1 FEBRUARY 1964

The Applicability of the Third Integral Of Motion: Some Numerical Experiments

MICHEL HÉNON* AND CARL HEILES

Princeton University Observatory, Princeton, New Jersey

(Received 7 August 1963)

The problem of the existence of a third isolating integral of motion in an axisymmetric potential is investigated by numerical experiments. It is found that the third integral exists for only a limited range of initial conditions.

Example (Hénon-Heiles system)

$$H = \frac{1}{2}\left(p_x^2 + p_y^2\right) + \frac{1}{2}\left(x^2 + y^2\right) + x^2 y - \frac{1}{3} y^3$$

THE ASTRONOMICAL JOURNAL VOLUME 69, NUMBER 1 FEBRUARY 1964

The Applicability of the Third Integral Of Motion: Some Numerical Experiments

MICHEL HÉNON* AND CARL HEILES

Princeton University Observatory, Princeton, New Jersey

(Received 7 August 1963)

The problem of the existence of a third isolating integral of motion in an axisymmetric potential is investigated by numerical experiments. It is found that the third integral exists for only a limited range of initial conditions.

Hamilton's equations of motion:

$$\frac{dp_i}{dt} = -\frac{\partial H}{\partial q_i}, \quad \frac{dq_i}{dt} = \frac{\partial H}{\partial p_i}$$

Example (Hénon-Heiles system)

$$H = \frac{1}{2}\left(p_x^2 + p_y^2\right) + \frac{1}{2}\left(x^2 + y^2\right) + x^2 y - \frac{1}{3}y^3$$

THE ASTRONOMICAL JOURNAL VOLUME 69, NUMBER 1 FEBRUARY 1964

The Applicability of the Third Integral Of Motion: Some Numerical Experiments

Michel Hénon* and Carl Heiles

Princeton University Observatory, Princeton, New Jersey

(Received 7 August 1963)

The problem of the existence of a third isolating integral of motion in an axisymmetric potential is investigated by numerical experiments. It is found that the third integral exists for only a limited range of initial conditions.

Hamilton's equations of motion:

$$\frac{dp_i}{dt} = -\frac{\partial H}{\partial q_i}, \quad \frac{dq_i}{dt} = \frac{\partial H}{\partial p_i} \Rightarrow \begin{cases} \dot{x} = p_x \\ \dot{y} = p_y \\ \dot{p}_x = -x - 2xy \\ \dot{p}_y = -y - x^2 + y^2 \end{cases}$$

Chaos

Definition [Devaney (1989)]

Let V be a set and $f : V \to V$ a map on this set.

We say that f is chaotic on V if

1. **f has sensitive dependence on initial conditions.**
2. **f is topologically transitive.**
3. **periodic points are dense in V.**

Usually, in physics and applied sciences, people use the notion of chaos in relation to the sensitive dependence on initial conditions.

Regular vs Chaotic orbits

Hénon-Heiles system

$$H = \frac{1}{2}\left(p_x^2 + p_y^2\right) + \frac{1}{2}\left(x^2 + y^2\right) + x^2 y - \frac{1}{3}y^3$$

Regular vs Chaotic orbits

Hénon-Heiles system

$$H = \frac{1}{2}\left(p_x^2 + p_y^2\right) + \frac{1}{2}\left(x^2 + y^2\right) + x^2 y - \frac{1}{3} y^3$$

For H=0.125 we get a regular and a chaotic orbit with initial conditions (ICs):

$x=0$, $y=0.1$, $p_y=0$ and **$x=0$, $y=-0.25$, $p_y=0$.**

Regular vs Chaotic orbits

Hénon-Heiles system

$$H = \frac{1}{2}\left(p_x^2 + p_y^2\right) + \frac{1}{2}\left(x^2 + y^2\right) + x^2 y - \frac{1}{3} y^3$$

For H=0.125 we get a regular and a chaotic orbit with initial conditions (ICs):

$x=0$, $y=0.1$, $p_y=0$ and **$x=0$, $y=-0.25$, $p_y=0$.**

We perturb both ICs by **$\delta p_y=10^{-11}$** (!) and check the evolution of x

Regular vs Chaotic orbits

Hénon-Heiles system

$$H = \frac{1}{2}\left(p_x^2 + p_y^2\right) + \frac{1}{2}\left(x^2 + y^2\right) + x^2 y - \frac{1}{3}y^3$$

For H=0.125 we get a regular and a chaotic orbit with initial conditions (ICs):

$x=0, y=0.1, p_y=0$ and **$x=0, y=-0.25, p_y=0.$**

We perturb both ICs by **$\delta p_y=10^{-11}$** (!) and check the evolution of x

Orbit **Perturbed**

Regular vs Chaotic orbits

Hénon-Heiles system

$$H = \frac{1}{2}\left(p_x^2 + p_y^2\right) + \frac{1}{2}\left(x^2 + y^2\right) + x^2 y - \frac{1}{3}y^3$$

For H=0.125 we get a regular and a chaotic orbit with initial conditions (ICs):

$x=0$, $y=0.1$, $p_y=0$ and **$x=0$, $y=-0.25$, $p_y=0$.**

We perturb both ICs by **$\delta p_y=10^{-11}$** (!) and check the evolution of x

		Orbit	**Perturbed**
t=	100	x= 0.13299571833307644	0.13299571833727063064

Regular vs Chaotic orbits

Hénon-Heiles system

$$H = \frac{1}{2}\left(p_x^2 + p_y^2\right) + \frac{1}{2}\left(x^2 + y^2\right) + x^2 y - \frac{1}{3} y^3$$

For H=0.125 we get a regular and a chaotic orbit with initial conditions (ICs):

$x=0$, $y=0.1$, $p_y=0$ and **$x=0$, $y=-0.25$, $p_y=0$.**

We perturb both ICs by **$\delta p_y=10^{-11}$** (!) and check the evolution of x

			Orbit	**Perturbed**
t=	100	x=	0.13299571833307644	0.13299571833 7263064
t=	5000	x=	0.37699928389102310	0.37699928387 0156576

Regular vs Chaotic orbits

Hénon-Heiles system

$$H = \frac{1}{2}\left(p_x^2 + p_y^2\right) + \frac{1}{2}\left(x^2 + y^2\right) + x^2 y - \frac{1}{3} y^3$$

For H=0.125 we get a regular and a chaotic orbit with initial conditions (ICs):

$x=0$, $y=0.1$, $p_y=0$ and **$x=0$, $y=-0.25$, $p_y=0$.**

We perturb both ICs by **$\delta p_y=10^{-11}$** (!) and check the evolution of x

		Orbit	**Perturbed**
t=	100	x= 0.13299571833307644	0.132995718337263064
t=	5000	x= 0.37699928389102310	0.376999283870156576
t=	10000	x=-0.159094583356855224	-0.159094583341260309

Regular vs Chaotic orbits

Hénon-Heiles system

$$H = \frac{1}{2}\left(p_x^2 + p_y^2\right) + \frac{1}{2}\left(x^2 + y^2\right) + x^2 y - \frac{1}{3}y^3$$

For H=0.125 we get a regular and a chaotic orbit with initial conditions (ICs):

$x=0, y=0.1, p_y=0$ and **$x=0, y=-0.25, p_y=0.$**

We perturb both ICs by **$\delta p_y=10^{-11}$** (!) and check the evolution of x

		Orbit	**Perturbed**
t=	100	x= 0.13299571833307644	0.13299571833737263064
t=	5000	x= 0.376999283889102310	0.376999283870156576
t=	10000	x=-0.159094583356855224	-0.159094583341260309
t=	50000	x= 0.101992400739955760	0.101992400253961321

Regular vs Chaotic orbits

Hénon-Heiles system

$$H = \frac{1}{2}\left(p_x^2 + p_y^2\right) + \frac{1}{2}\left(x^2 + y^2\right) + x^2 y - \frac{1}{3}y^3$$

For H=0.125 we get a regular and a chaotic orbit with initial conditions (ICs):

$x=0, y=0.1, p_y=0$ and **$x=0, y=-0.25, p_y=0.$**

We perturb both ICs by **$\delta p_y=10^{-11}$** (!) and check the evolution of x

		Orbit	**Perturbed**
t=	100	x= 0.13299571833307644	0.13299571833707263064
t=	5000	x= 0.37699928389102310	0.37699928370156576
t=	10000	x=-0.15909458335 6855224	-0.15909458334 1260309
t=	50000	x= 0.10199240073 9955760	0.10199240025 3961321
t=	100000	x=-0.38112053374 6511780	-0.38112053332 7258870

Regular vs Chaotic orbits

Hénon-Heiles system

$$H = \frac{1}{2}\left(p_x^2 + p_y^2\right) + \frac{1}{2}\left(x^2 + y^2\right) + x^2 y - \frac{1}{3}y^3$$

For H=0.125 we get a regular and a chaotic orbit with initial conditions (ICs):

$x=0, y=0.1, p_y=0$ and **$x=0, y=-0.25, p_y=0.$**

We perturb both ICs by **$\delta p_y=10^{-11}$** (!) and check the evolution of x

	Orbit	Perturbed
t= 100	x= 0.13299571833307644	0.13299571833726306
t= 5000	x= 0.37699928389102310	0.37699928370156576
t= 10000	x=-0.15909458335685522	-0.15909458334126030
t= 50000	x= 0.10199240073995576	0.10199240025396132
t=100000	x=-0.38112053374651178	-0.38112053332725887
t= 100	x= 0.09027281773516783	0.09027282135576866

Regular vs Chaotic orbits

Hénon-Heiles system

$$H = \frac{1}{2}\left(p_x^2 + p_y^2\right) + \frac{1}{2}\left(x^2 + y^2\right) + x^2 y - \frac{1}{3}y^3$$

For H=0.125 we get a regular and a chaotic orbit with initial conditions (ICs):

$x=0, y=0.1, p_y=0$ and **$x=0, y=-0.25, p_y=0$.**

We perturb both ICs by **$\delta p_y=10^{-11}$** (!) and check the evolution of x

		Orbit	Perturbed
t= 100	x=	0.13299571833307644	0.13299571833727263064
t= 5000	x=	0.37699928389102310	0.37699928370156576
t= 10000	x=	-0.15909458335685524	-0.15909458334126030 9
t= 50000	x=	0.10199240073995576 0	0.10199240025396132 1
t=100000	x=	-0.38112053374651178 0	-0.38112053332725887 0
t= 100	x=	0.09027281773516783 5	0.09027282135576866 8
t= 200	x=	0.29503168748224928 3	0.29503188485862563 7

Regular vs Chaotic orbits

Hénon-Heiles system

$$H = \frac{1}{2}\left(p_x^2 + p_y^2\right) + \frac{1}{2}\left(x^2 + y^2\right) + x^2 y - \frac{1}{3}y^3$$

For H=0.125 we get a regular and a chaotic orbit with initial conditions (ICs):

$x=0$, $y=0.1$, $p_y=0$ and **$x=0$, $y=-0.25$, $p_y=0$.**

We perturb both ICs by **$\delta p_y=10^{-11}$** (!) and check the evolution of x

		Orbit	**Perturbed**
t=	100	x= 0.13299571833307644	0.13299571833737263064
t=	5000	x= 0.37699928389102310	0.37699928370156576
t=	10000	x=-0.159094583356855224	-0.159094583341260309
t=	50000	x= 0.101992400739955760	0.101992400253961321
t=	100000	x=-0.381120533746511780	-0.381120533327258870
t=	100	x= 0.090272817735167835	0.090272821355768668
t=	200	x= 0.295031687482249283	0.295031884858625637
t=	300	x= 0.515226330109450181	0.515225440480693297

Regular vs Chaotic orbits

Hénon-Heiles system

$$H = \frac{1}{2}\left(p_x^2 + p_y^2\right) + \frac{1}{2}\left(x^2 + y^2\right) + x^2 y - \frac{1}{3}y^3$$

For H=0.125 we get a regular and a chaotic orbit with initial conditions (ICs):

$x=0, y=0.1, p_y=0$ and **$x=0, y=-0.25, p_y=0.$**

We perturb both ICs by $\delta p_y=10^{-11}$ (!) and check the evolution of x

	Orbit	**Perturbed**
t= 100	x= 0.13299571833307644	0.13299571833707263064
t= 5000	x= 0.37699928389102310	0.37699928370156576
t= 10000	x=-0.15909458335685522 4	-0.15909458334126030 9
t= 50000	x= 0.10199240073995576 0	0.10199240025396132 1
t=100000	x=-0.38112053374651178 0	-0.38112053332725887 0
t= 100	x= 0.09027281773516783 5	0.09027282135576866 8
t= 200	x= 0.29503168748224928 3	0.29503188485862563 7
t= 300	x= 0.51522633010945018 1	0.51522544048069329 7
t= 400	x= 0.06344188934742586 7	0.06135955855100834 5

Regular vs Chaotic orbits

Hénon-Heiles system

$$H = \frac{1}{2}\left(p_x^2 + p_y^2\right) + \frac{1}{2}\left(x^2 + y^2\right) + x^2 y - \frac{1}{3}y^3$$

For H=0.125 we get a regular and a chaotic orbit with initial conditions (ICs):

$x=0, y=0.1, p_y=0$ and **$x=0, y=-0.25, p_y=0$.**

We perturb both ICs by **$\delta p_y=10^{-11}$** (!) and check the evolution of x

t		**Orbit**	**Perturbed**
t= 100	x=	0.13299571833307644	0.13299571833726306
t= 5000	x=	0.37699928389102310	0.37699928370156576
t= 10000	x=	-0.15909458335685522	-0.15909458334126030
t= 50000	x=	0.10199240073995576	0.10199240025396132
t=100000	x=	-0.38112053374651178	-0.38112053332725887
t= 100	x=	0.09027281773516783	0.09027282135576866
t= 200	x=	0.29503168748224928	0.29503188485862563
t= 300	x=	0.51522633010945018	0.51522544048069329
t= 400	x=	0.06344188934742586	0.06135955855100834
t= 500	x=	0.07835771929052352	-0.27081102267434109

Regular vs Chaotic orbits

Chaotic orbit

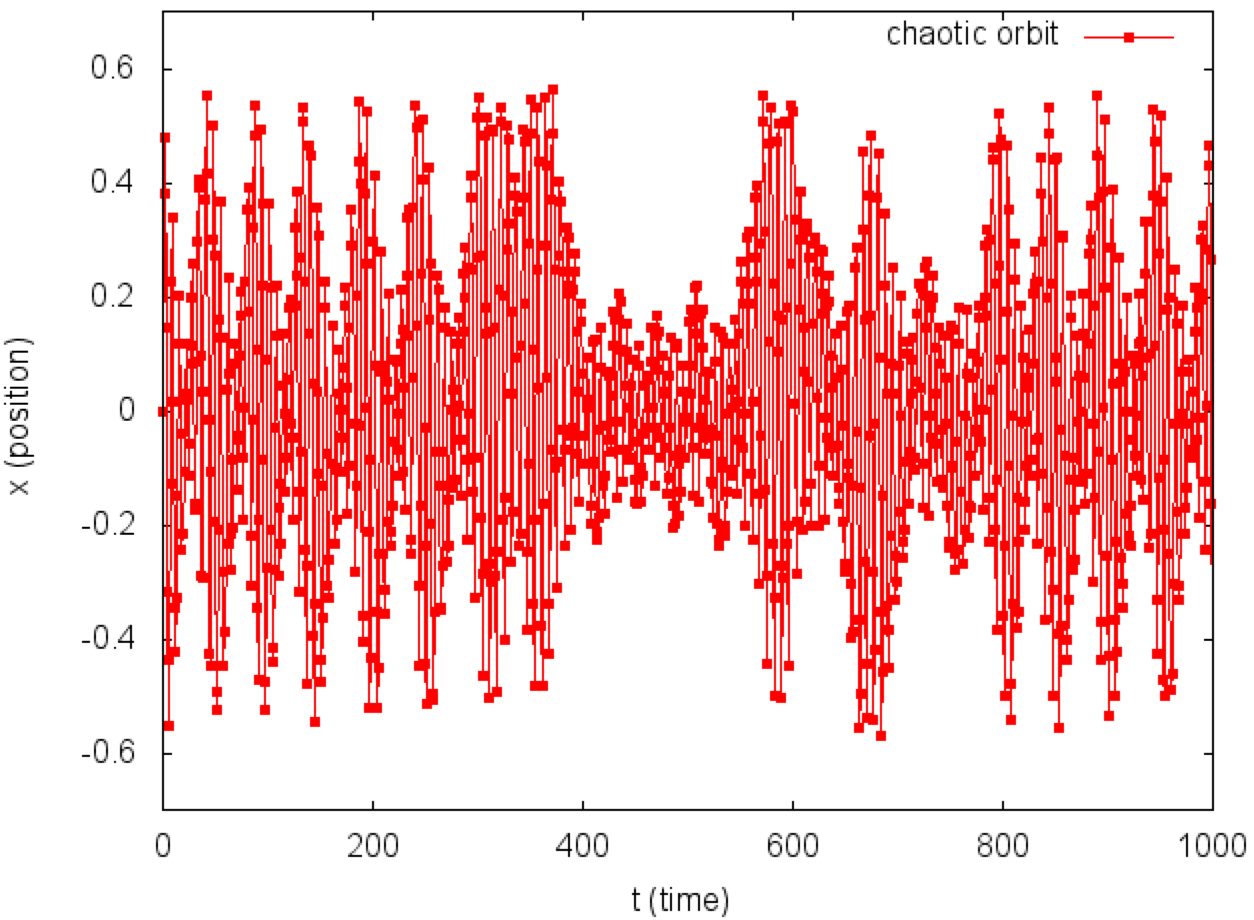

Regular vs Chaotic orbits

Chaotic orbit and its perturbation

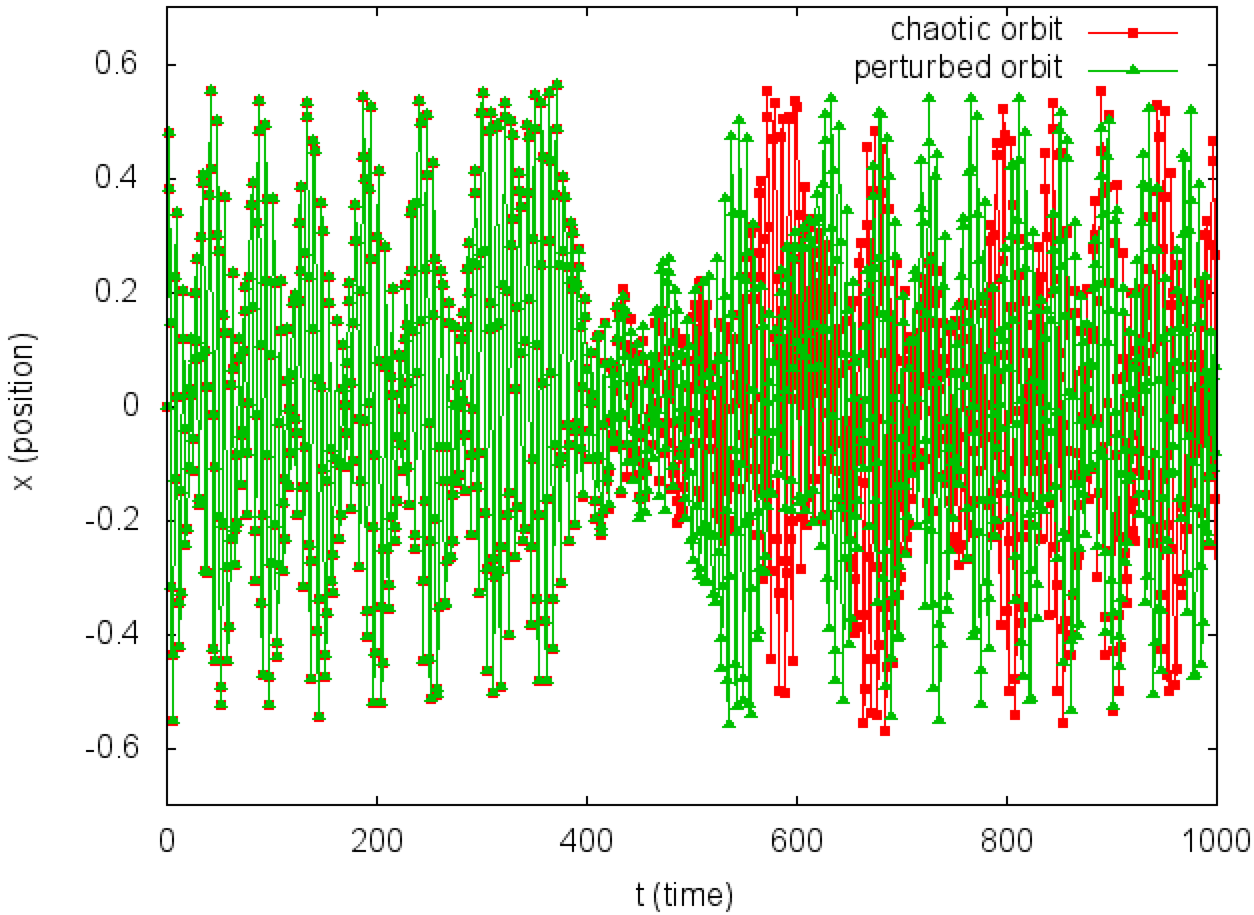

Regular vs Chaotic orbits

Regular orbit

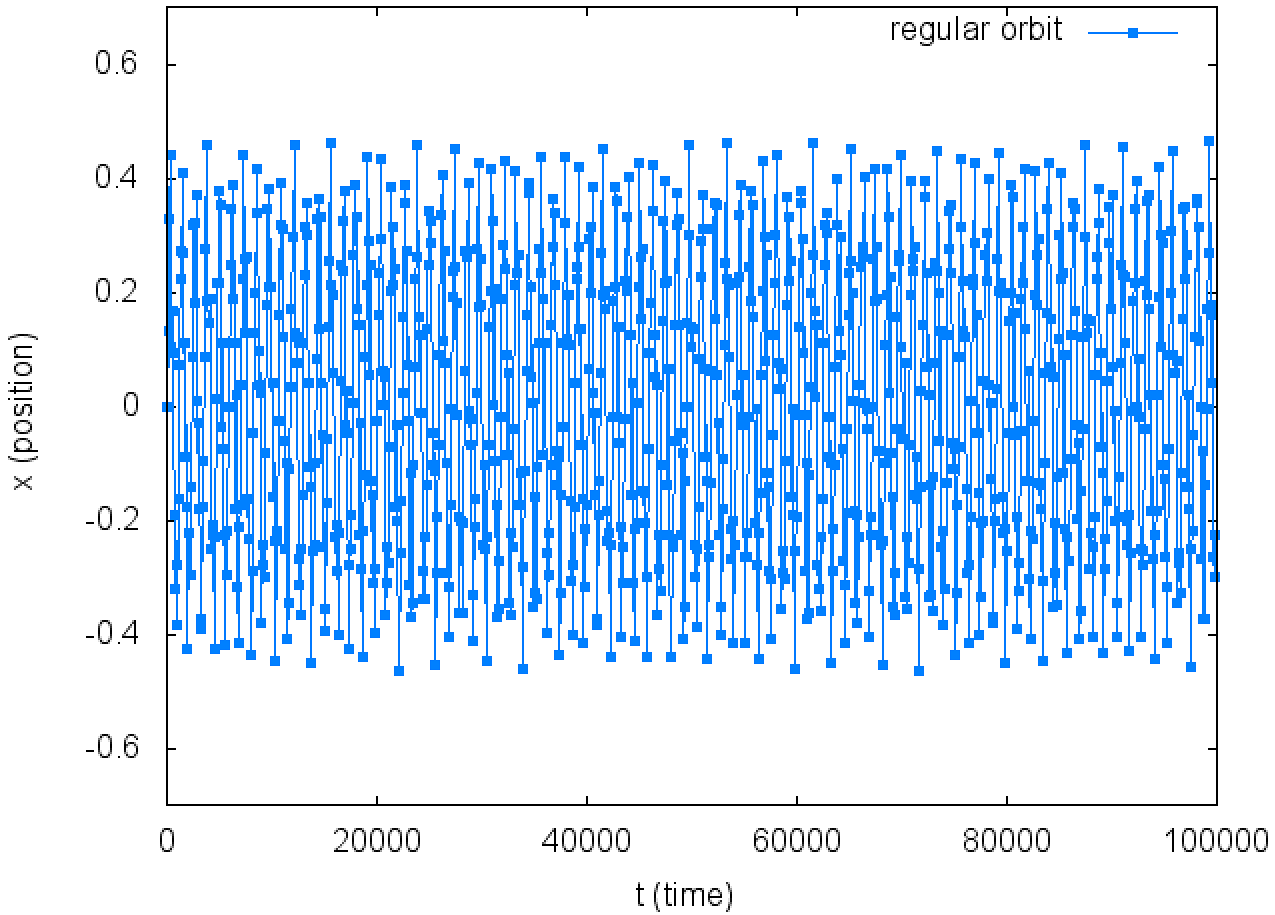

Regular vs Chaotic orbits

Regular orbit and its perturbation

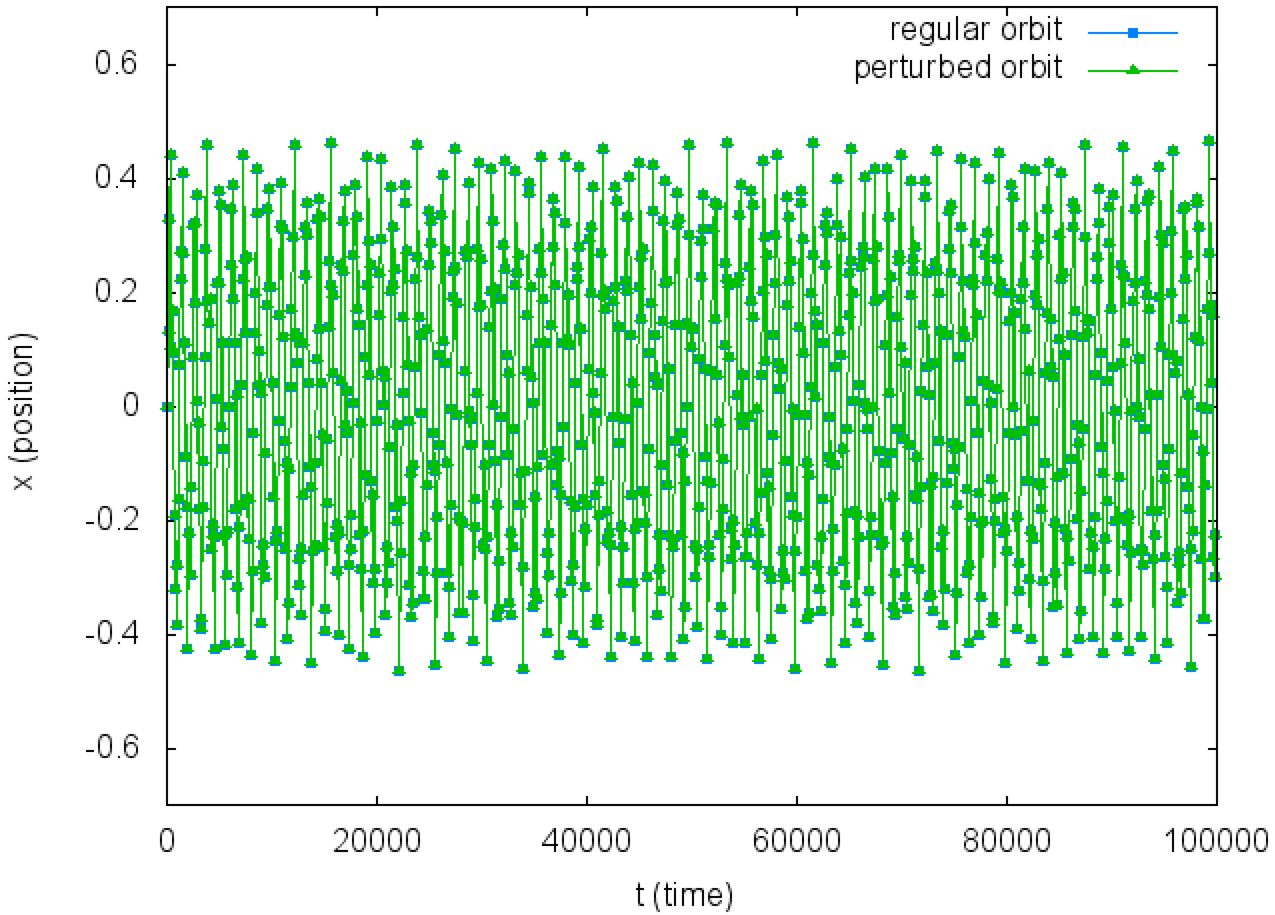

Chaos detection techniques

- **Based on the visualization of orbits**
  - ✓ **Poincaré Surface of Section (PSS)**
  - ✓ **the color and rotation (CR) method**
  - ✓ **the 3D phase space slices (3PSS) technique**

Poincaré Surface of Section (PSS)

We can constrain the study of an N+1 degree of freedom Hamiltonian system to a 2N-dimensional subspace of the general phase space.

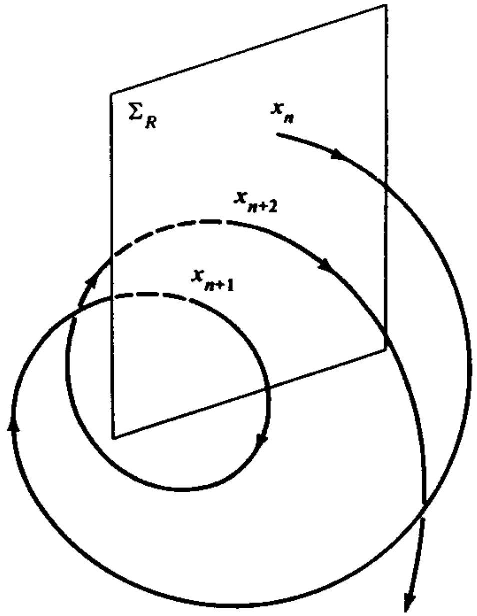

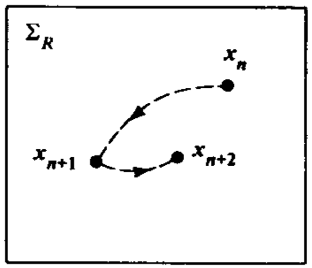

Lieberman & Lichtenberg, 1992, *Regular and Chaotic Dynamics*, Springer.

Poincaré Surface of Section (PSS)

We can constrain the study of an N+1 degree of freedom Hamiltonian system to a 2N-dimensional subspace of the general phase space.

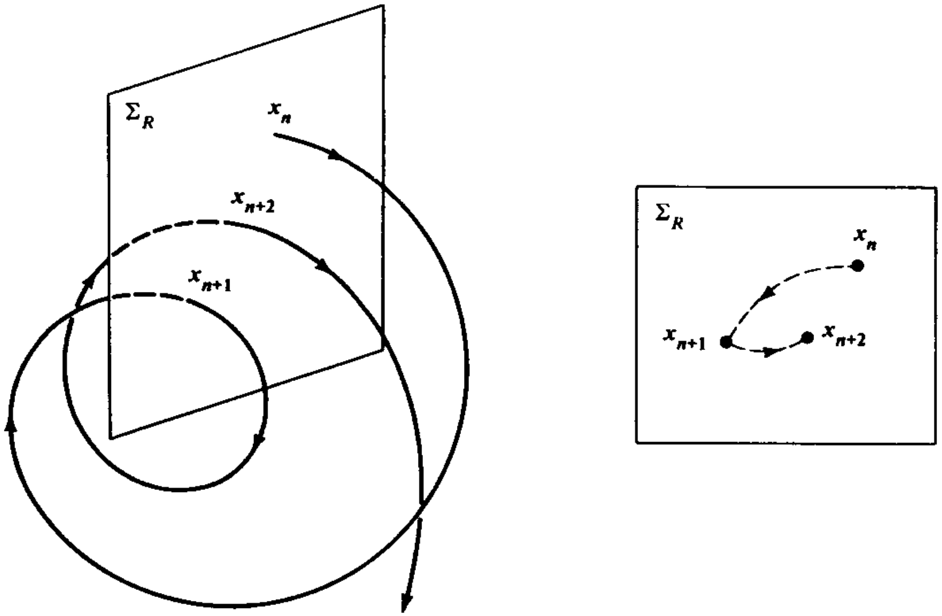

Lieberman & Lichtenberg, 1992, *Regular and Chaotic Dynamics*, Springer.

In general we can assume a PSS of the form q_{N+1}=constant. Then only variables $q_1,q_2,\ldots,q_N,p_1,p_2,\ldots,p_N$ are needed to describe the evolution of an orbit on the PSS, since p_{N+1} can be found from the Hamiltonian.

Poincaré Surface of Section (PSS)

We can constrain the study of an N+1 degree of freedom Hamiltonian system to a 2N-dimensional subspace of the general phase space.

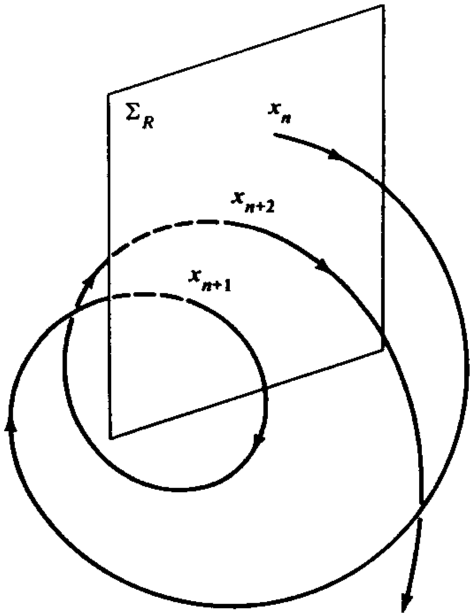

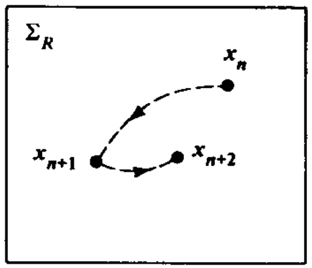

Lieberman & Lichtenberg, 1992, *Regular and Chaotic Dynamics*, Springer.

In general we can assume a PSS of the form q_{N+1}=constant. Then only variables $q_1, q_2, \ldots, q_N, p_1, p_2, \ldots, p_N$ are needed to describe the evolution of an orbit on the PSS, since p_{N+1} can be found from the Hamiltonian.

In this sense an N+1 degree of freedom Hamiltonian system corresponds to a 2N-dimensional map.

Hénon-Heiles system: PSS (x=0)

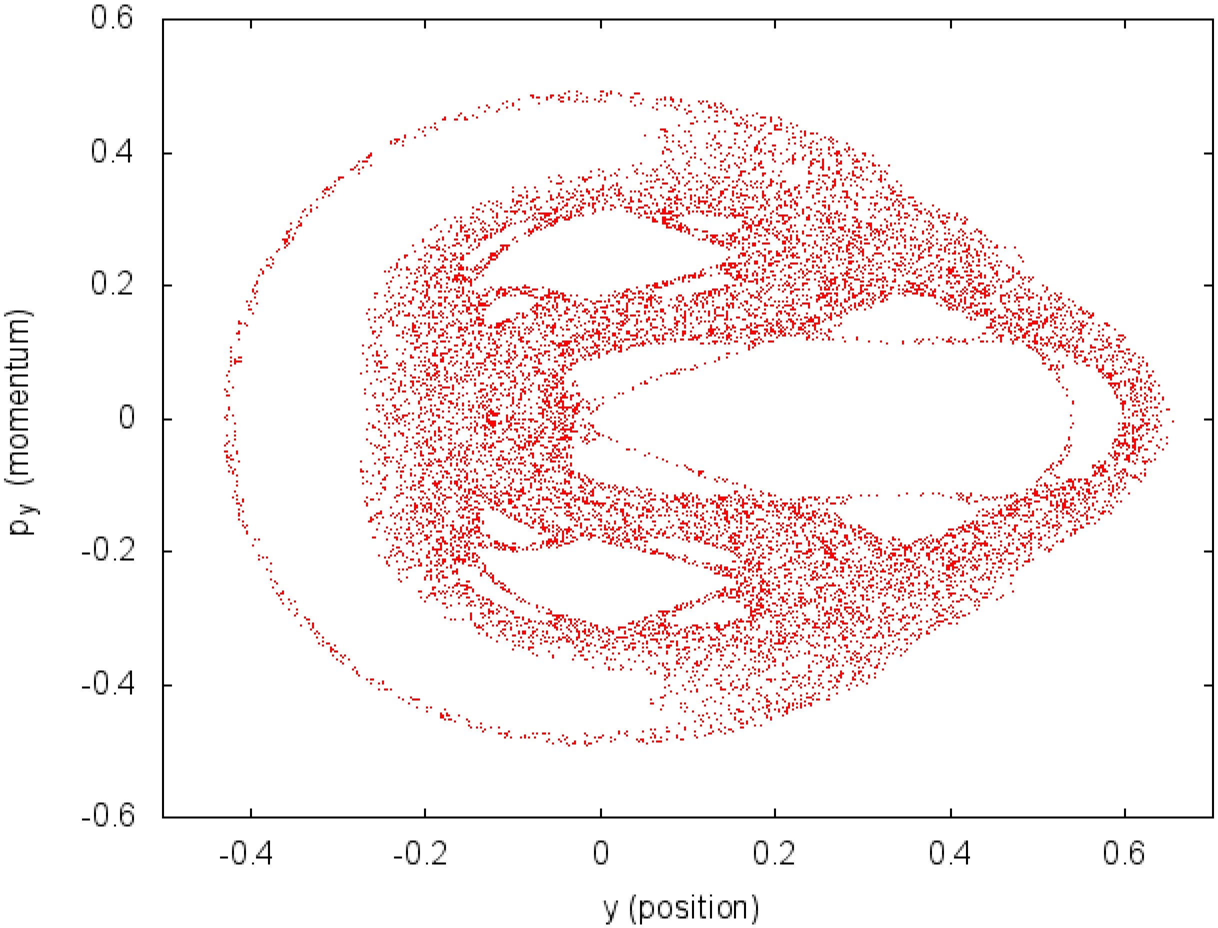

Chaotic orbit

Hénon-Heiles system: PSS (x=0)

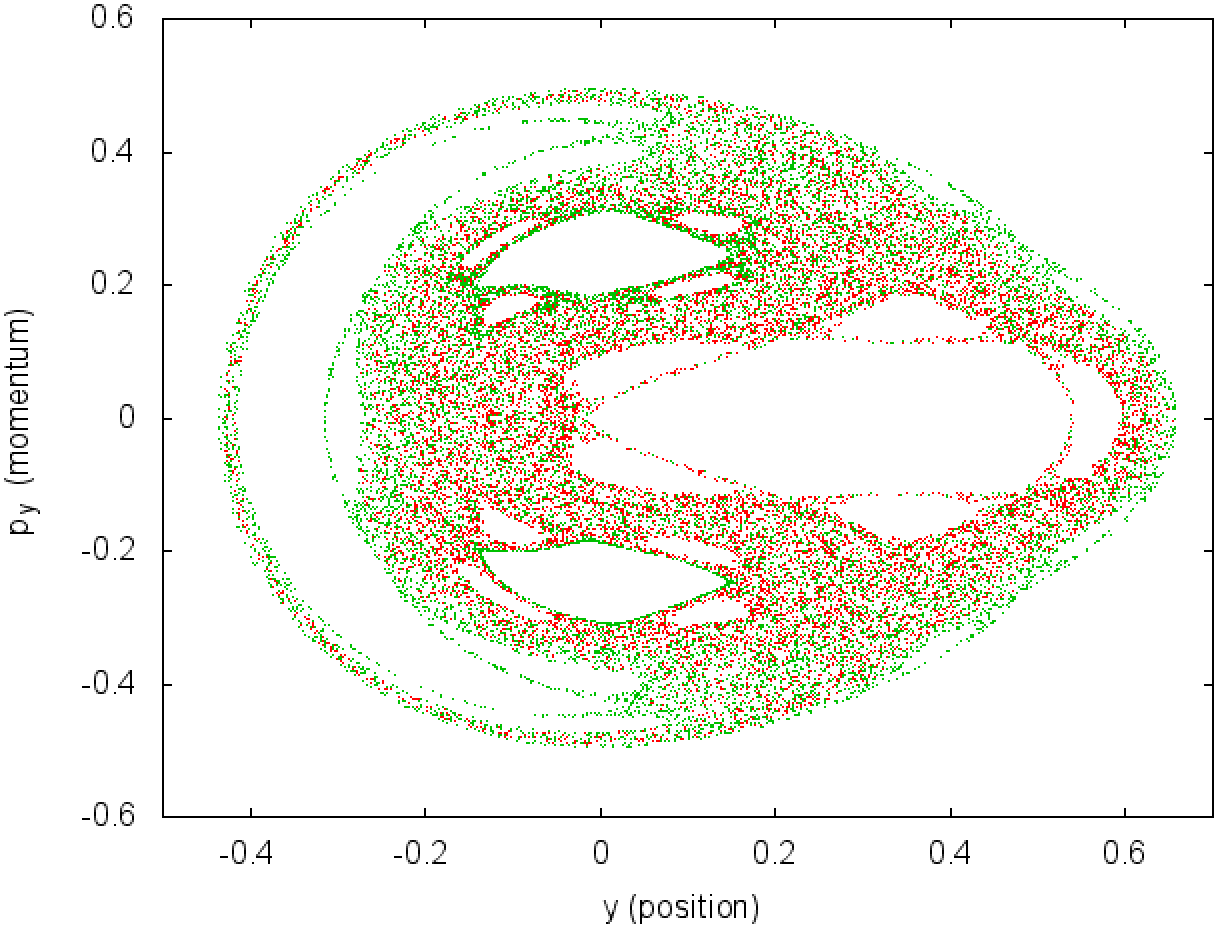

Chaotic orbit - Perturbed chaotic orbit

Hénon-Heiles system: PSS (x=0)

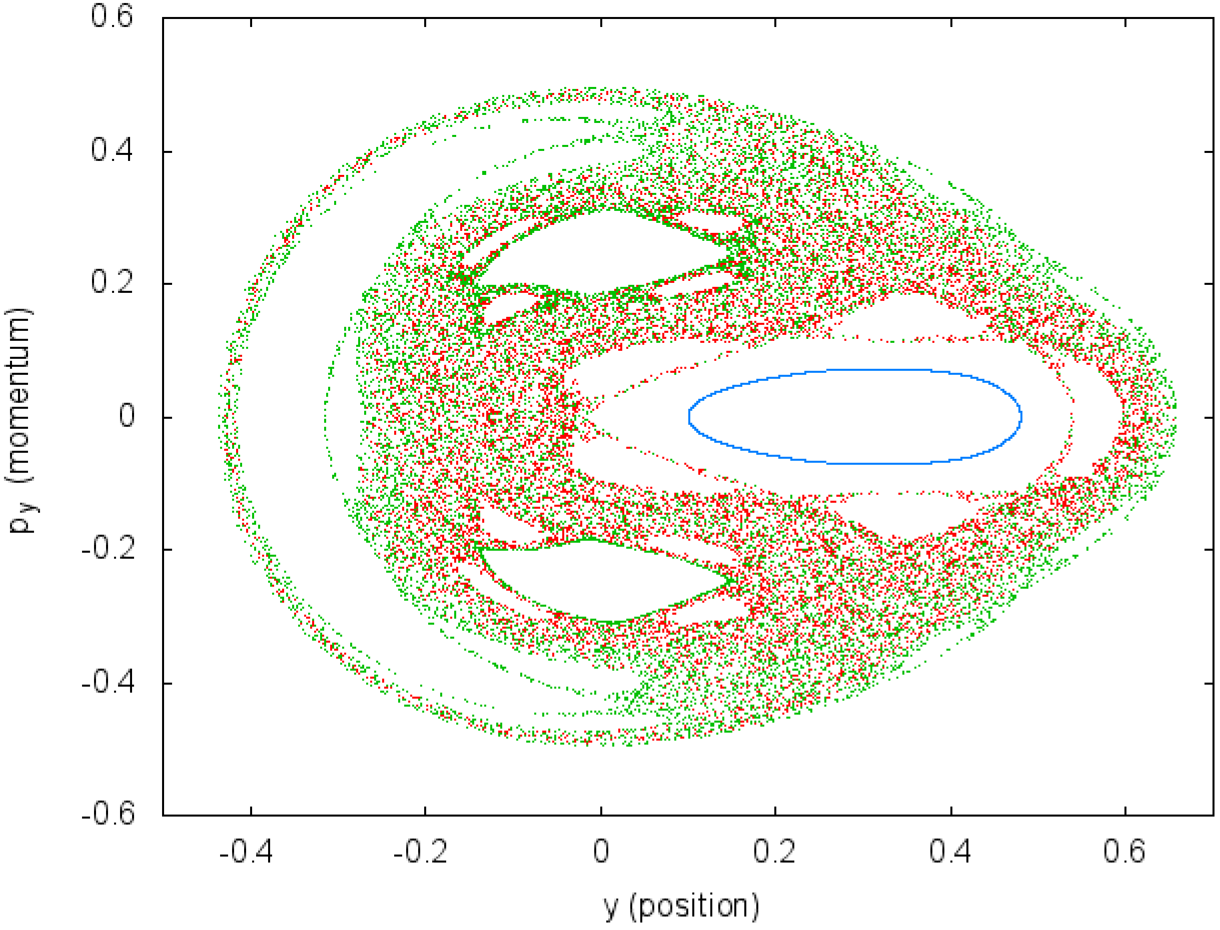

Chaotic orbit - Perturbed chaotic orbit

Regular orbit

Hénon-Heiles system: PSS (x=0)

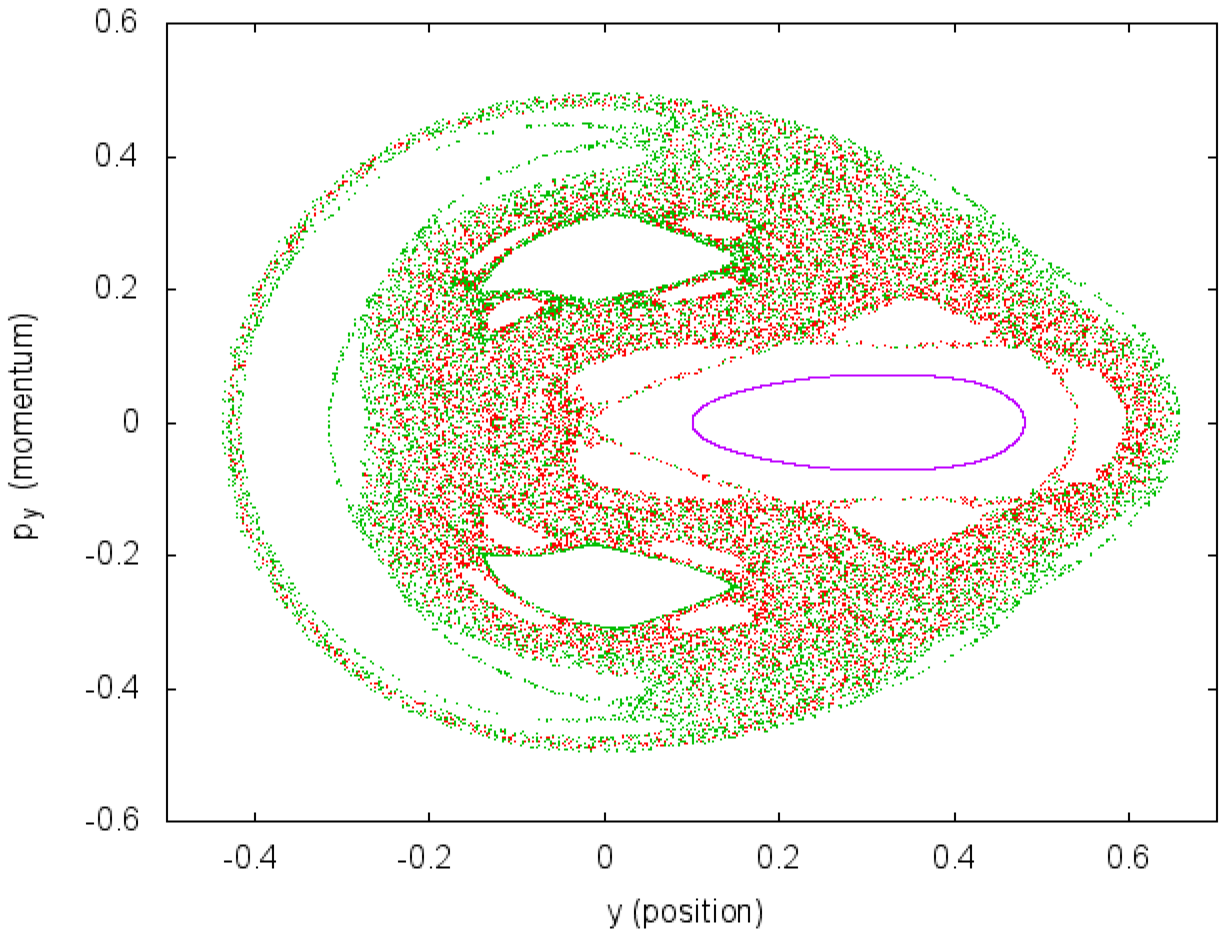

Chaotic orbit - Perturbed chaotic orbit

Regular orbit - Perturbed regular orbit

Hénon-Heiles system: PSS (x=0)

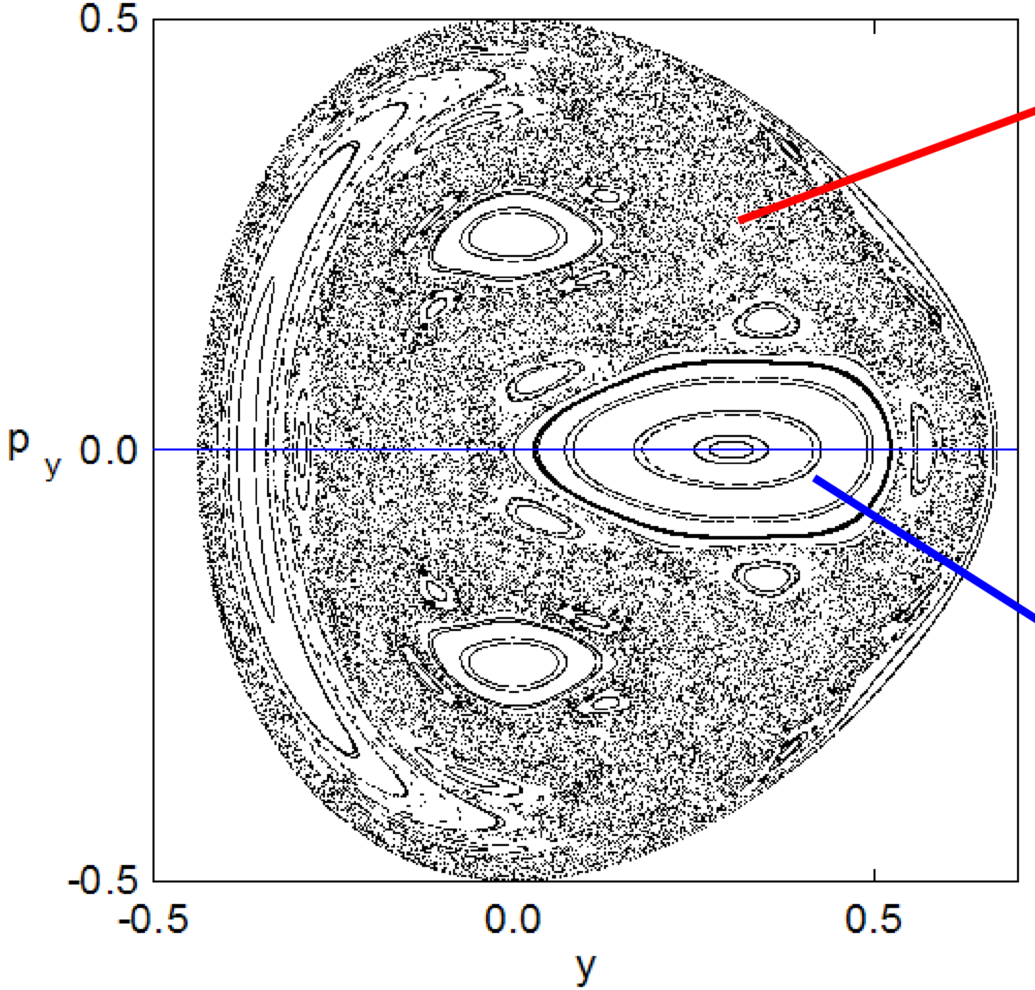

Chaotic motion
Chaotic sea

Regular motion
Island of stability

The color and rotation (CR) method

For 3 degree of freedom Hamiltonian systems and 4 dimensional symplectic maps:

We consider the 3D projection of the PSS and use color to indicate the 4th dimension.

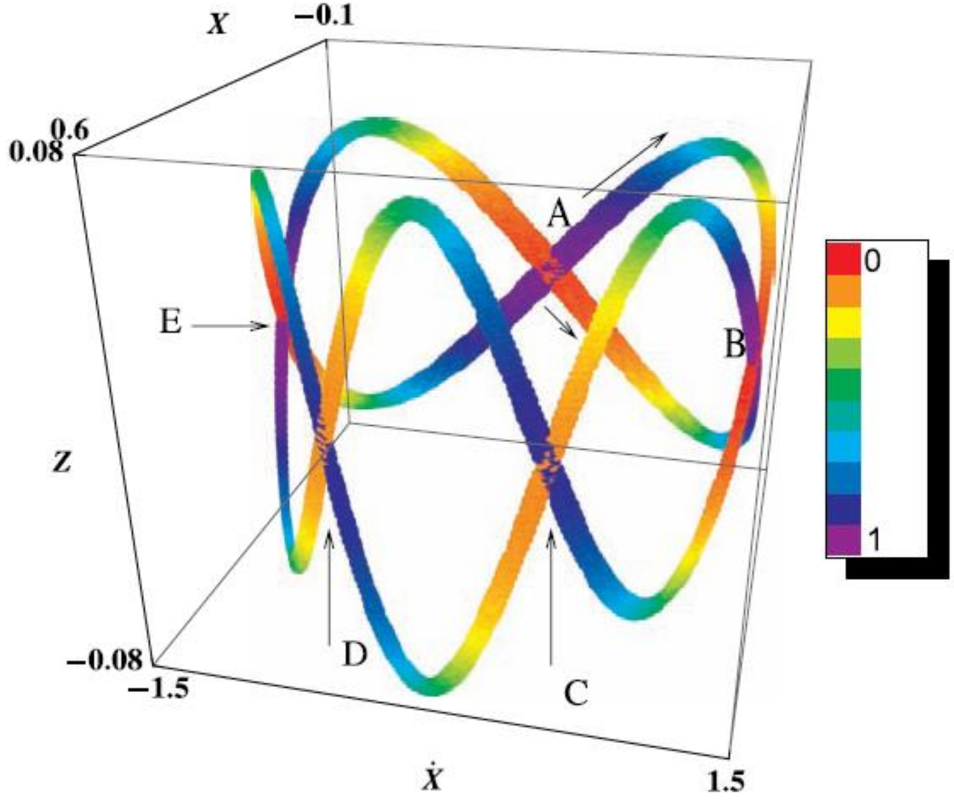

Katsanikas M and Patsis P A 2011 Int. J. Bif. Chaos 21 467

The 3D phase space slices (3PSS) technique

For 3 degree of freedom Hamiltonian systems and 4 dimensional symplectic maps:

We consider thin 3D phase space slices of the 4D phase space (e.g. $|p_2| \leq \varepsilon$) and present intersections of orbits with these slices.

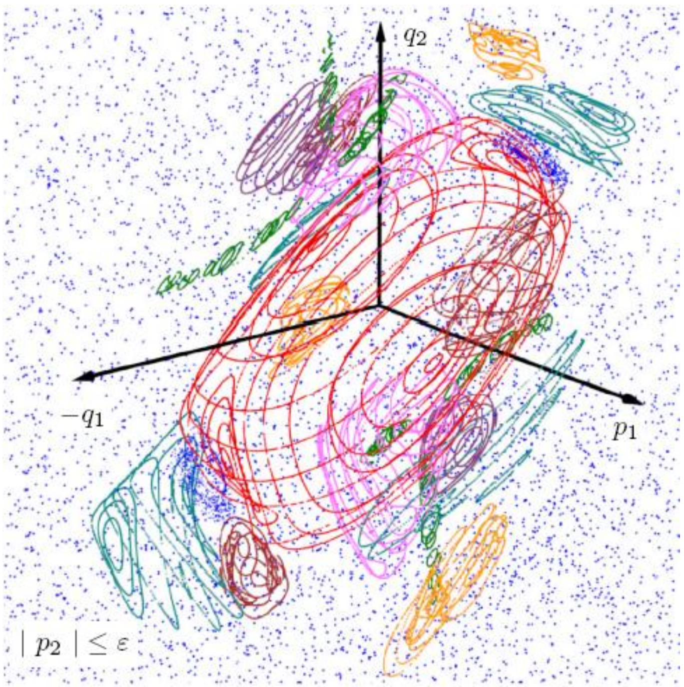

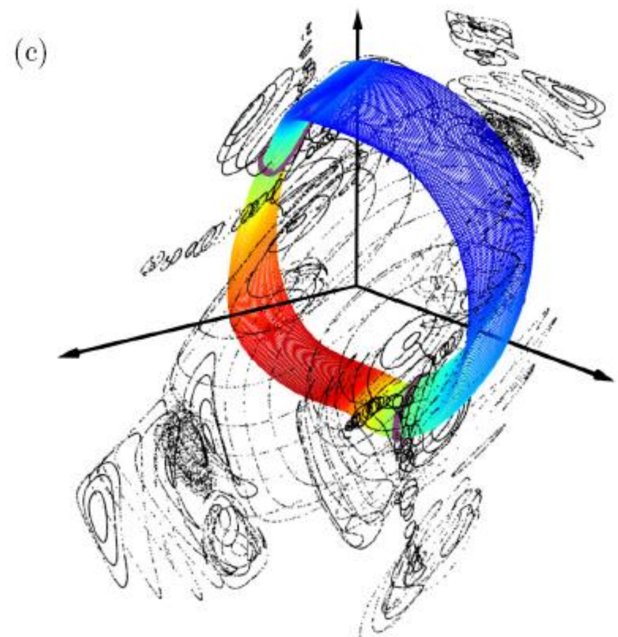

Richter et al. 2014 Phys. Rev. E 89 022902

Chaos detection techniques

- **Based on the visualization of orbits**
  - ✓ **Poincaré Surface of Section (PSS)**
  - ✓ **the color and rotation (CR) method**
  - ✓ **the 3D phase space slices (3PSS) technique**
- **Based on the numerical analysis of orbits**
  - ✓ **Frequency Map Analysis**
  - ✓ **0-1 test**

Frequency Map Analysis

Create Frequency Maps by computing the fundamental frequencies of orbits.

Regular motion: The computed frequencies do not vary in time

Chaotic motion: The computed frequencies vary in time

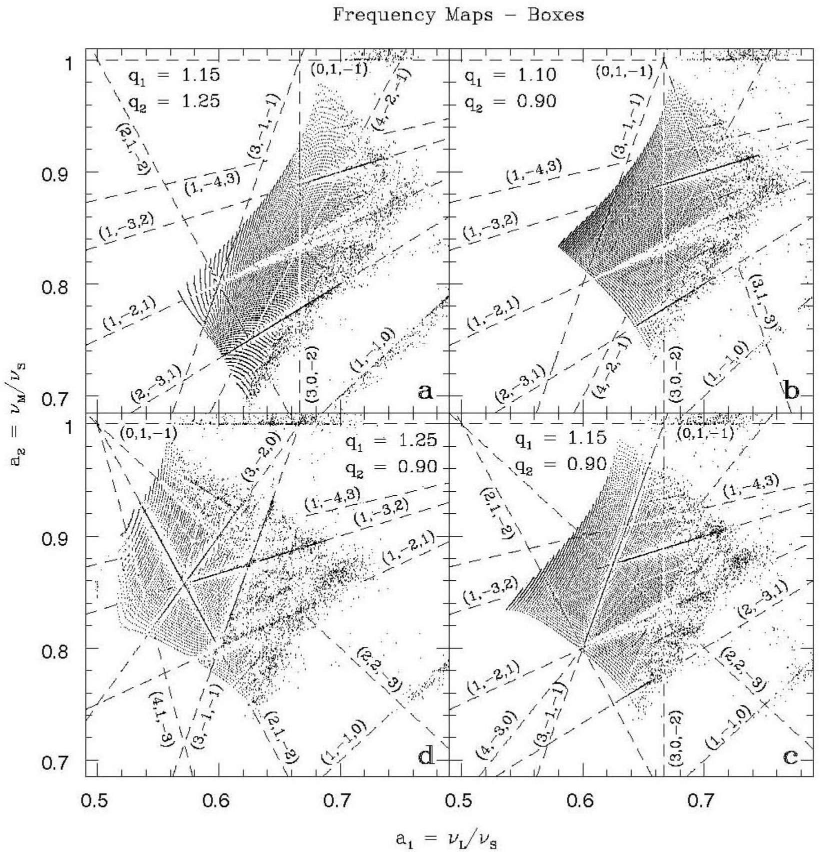

Papaphilippou Y and Laskar J 1998 Astron. Astrophys. 329 451

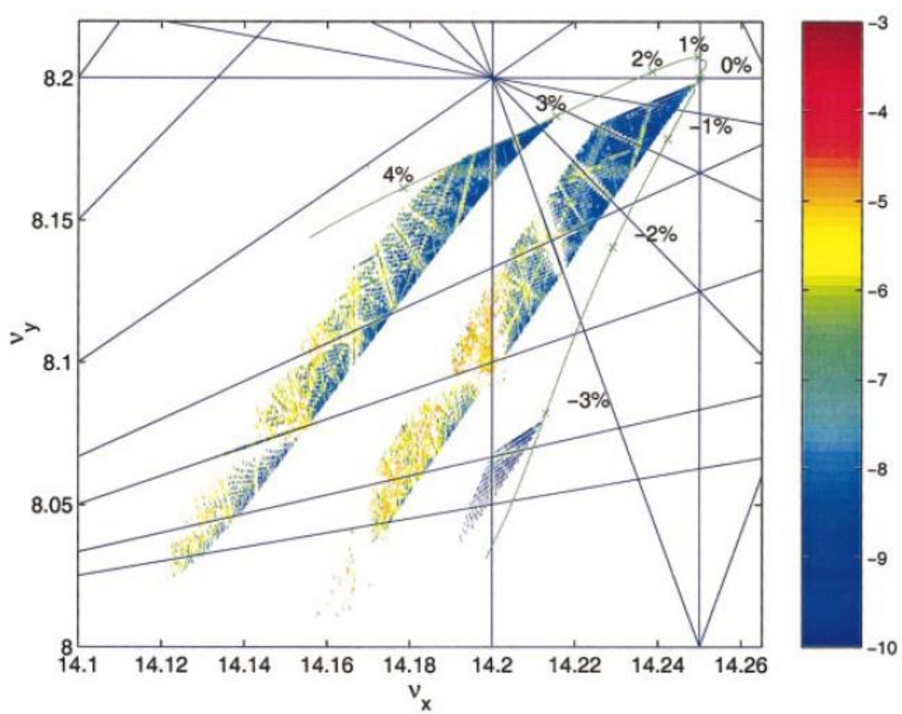

Steier C et al. 2002 Phys. Rev. E 65 056506

Chaos detection techniques

- **Based on the visualization of orbits**
  - ✓ **Poincaré Surface of Section (PSS)**
  - ✓ **the color and rotation (CR) method**
  - ✓ **the 3D phase space slices (3PSS) technique**
- **Based on the numerical analysis of orbits**
  - ✓ **Frequency Map Analysis**
  - ✓ **0-1 test**
- **Chaos indicators based on the evolution of deviation vectors from a given orbit**
  - ✓ **Maximum Lyapunov Exponent**
  - ✓ **Fast Lyapunov Indicator (FLI) and Orthogonal Fast Lyapunov Indicators (OFLI and OFLI2)**
  - ✓ **Mean Exponential Growth Factor of Nearby Orbits (MEGNO)**
  - ✓ **Relative Lyapunov Indicator (RLI)**
  - ✓ **Smaller ALignment Index – SALI**
  - ✓ **Generalized ALignment Index – GALI**

Variational Equations

We use the notation $\mathbf{x} = (q_1,q_2,\ldots,q_N,p_1,p_2,\ldots,p_N)^T$. The deviation vector from a given orbit is denoted by

$$\mathbf{v} = (\delta x_1, \delta x_2,\ldots,\delta x_n)^T \text{, with } n=2N$$

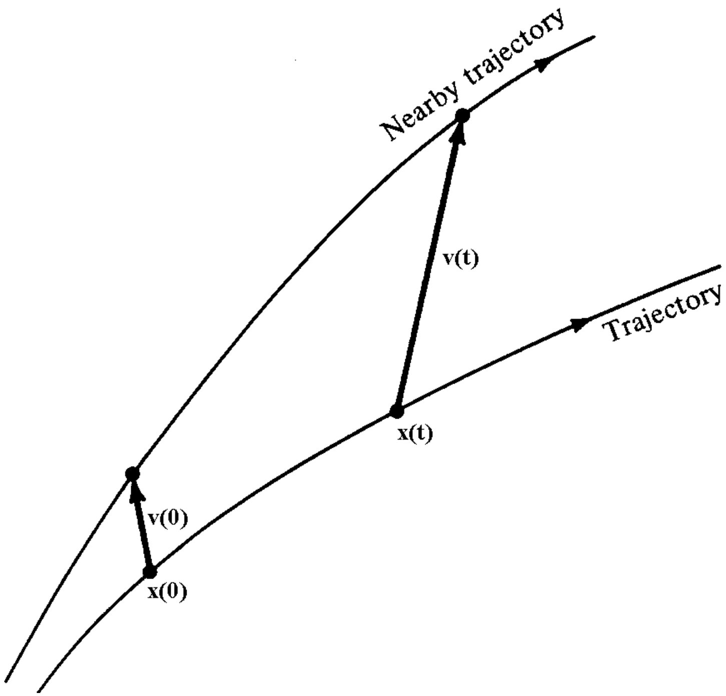

Benettin & Galgani, 1979, in Laval and Gressillon (eds.), op cit, 93

The time evolution of v is given by the so-called variational equations:

$$\frac{d\mathbf{v}}{dt} = -\mathbf{J}\cdot\mathbf{P}\cdot\mathbf{v}$$

where

$$\mathbf{J} = \begin{pmatrix} 0_N & -I_N \\ I_N & 0_N \end{pmatrix}, \quad P_{ij} = \frac{\partial^2 H}{\partial x_i \partial x_j} \quad i, j = 1, 2, \ldots, n$$

Symplectic Maps

Consider an 2N-dimensional symplectic map T. In this case we have discrete time.

The evolution of an orbit with initial condition

$$P(0)=(x_1(0), x_2(0),\ldots,x_{2N}(0))$$

is governed by the equations of map T

$$P(i+1)=T\,P(i)\ ,\ i=0,1,2,\ldots$$

The evolution of an initial deviation vector

$$v(0) = (\delta x_1(0), \delta x_2(0),\ldots, \delta x_{2N}(0))$$

is given by the corresponding tangent map

$$v(i+1) = \left.\frac{\partial T}{\partial P}\right|_i \cdot v(i)\ ,\ i = 0, 1, 2, \ldots$$

Maximum Lyapunov Exponent

Roughly speaking, the Lyapunov exponents of a given orbit characterize the mean exponential rate of divergence of trajectories surrounding it.

Consider an orbit in the 2N-dimensional phase space with initial condition x(0) and an initial deviation vector from it v(0). Then the mean exponential rate of divergence is:

$$mLCE = \sigma_1 = \lim_{t \to \infty} \frac{1}{t} \ln \frac{\left\| \vec{v}(t) \right\|}{\left\| \vec{v}(0) \right\|}$$

$\sigma_1 = 0 \rightarrow$ Regular motion

$\sigma_1 \neq 0 \rightarrow$ Chaotic motion

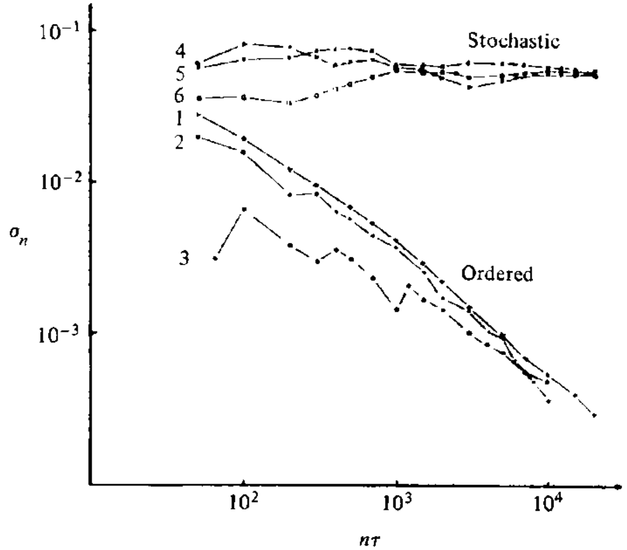

Figure 5.7. Behavior of σ_n at the intermediate energy $E = 0.125$ for initial points taken in the ordered (curves 1–3) or stochastic (curves 4–6) regions (after Benettin *et al.*, 1976).

If we start with more than one linearly independent deviation vectors they will align to the direction defined by the largest Lyapunov exponent for chaotic orbits.

Maximum Lyapunov Exponent

Hénon-Heiles system: Regular orbit

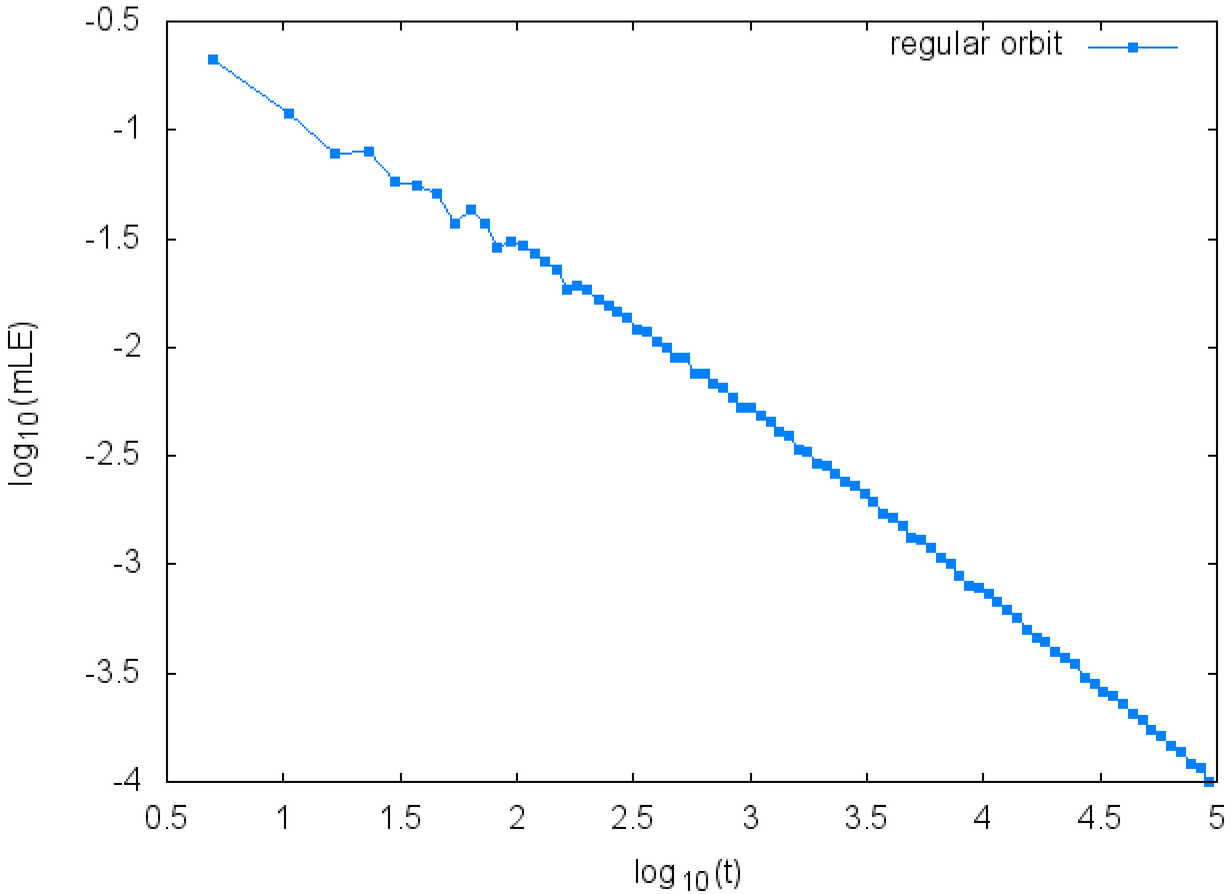

Maximum Lyapunov Exponent

Hénon-Heiles system: Regular orbit and Chaotic orbit

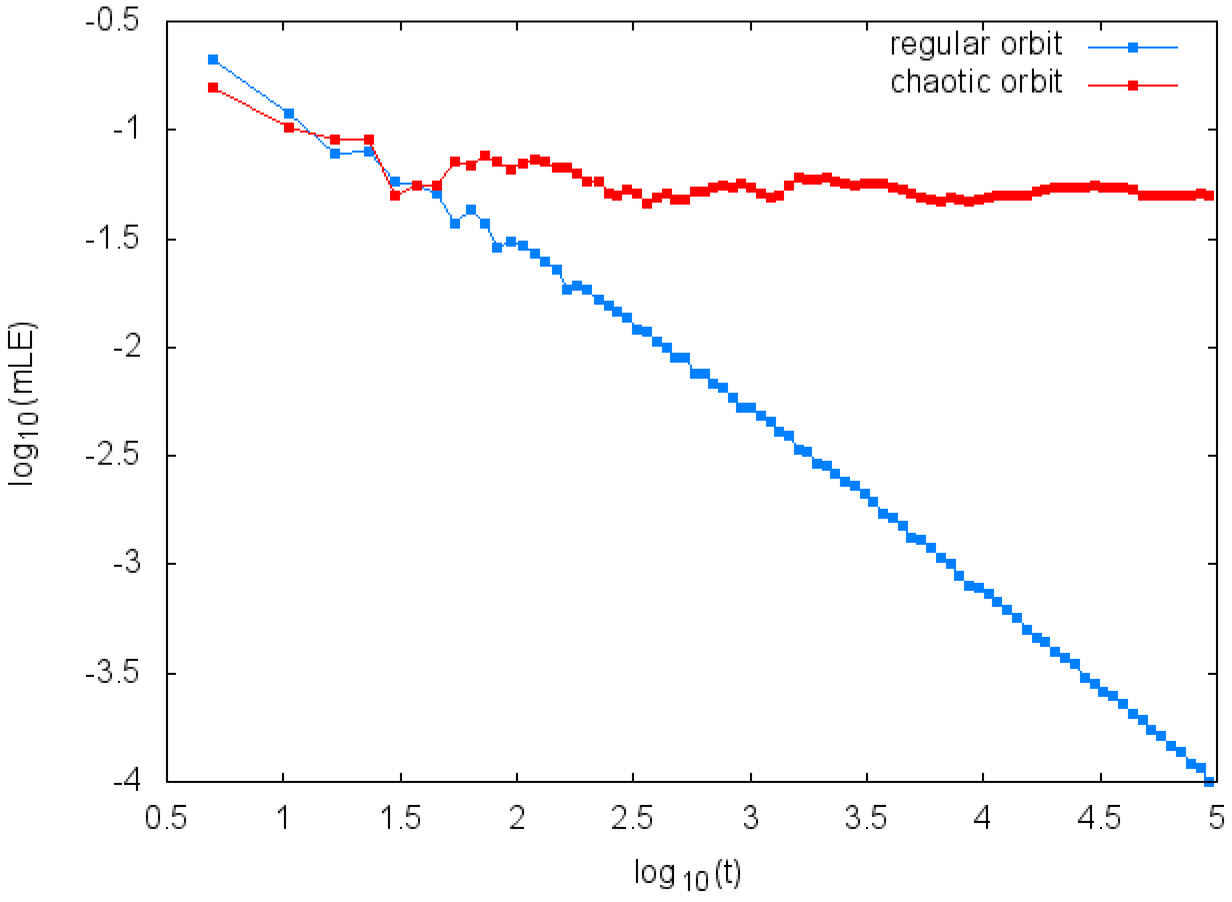

The
Smaller ALignment Index
(SALI)
method

Definition of the SALI

We follow the evolution in time of two different initial deviation vectors ($v_1(0)$, $v_2(0)$), and define the SALI (Ch.S. 2001, J. Phys. A) as:

$$SALI(t) = \min\left\{ \left\| \hat{v}_1(t) + \hat{v}_2(t) \right\|, \left\| \hat{v}_1(t) - \hat{v}_2(t) \right\| \right\}$$

where

$$\hat{v}_1(t) = \frac{v_1(t)}{\left\| v_1(t) \right\|}$$

When the two vectors become collinear

$$\mathbf{SALI(t) \rightarrow 0}$$

Behavior of the SALI for chaotic motion

For chaotic orbits the two initially different deviation vectors tend to coincide with the direction defined by the maximum Lyapunov exponent.

Behavior of the SALI for chaotic motion

For chaotic orbits the two initially different deviation vectors tend to coincide with the direction defined by the maximum Lyapunov exponent.

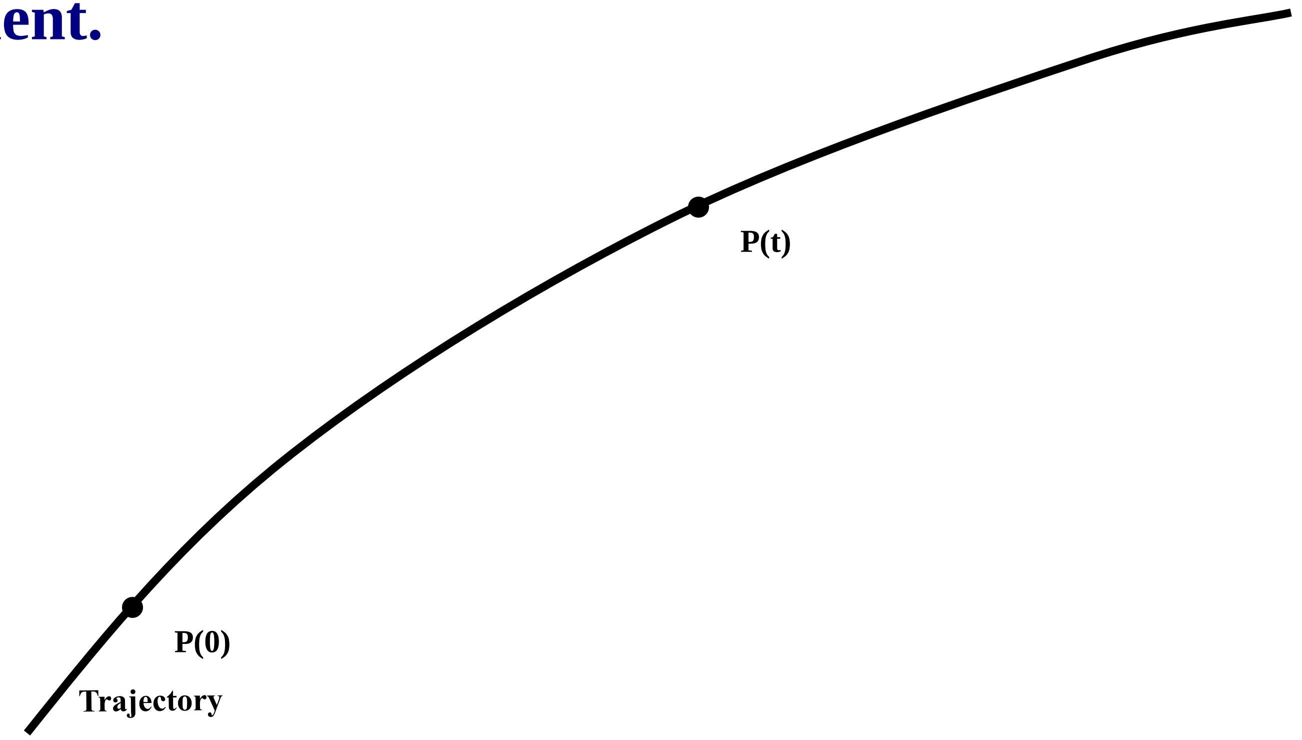

Behavior of the SALI for chaotic motion

For chaotic orbits the two initially different deviation vectors tend to coincide with the direction defined by the maximum Lyapunov exponent.

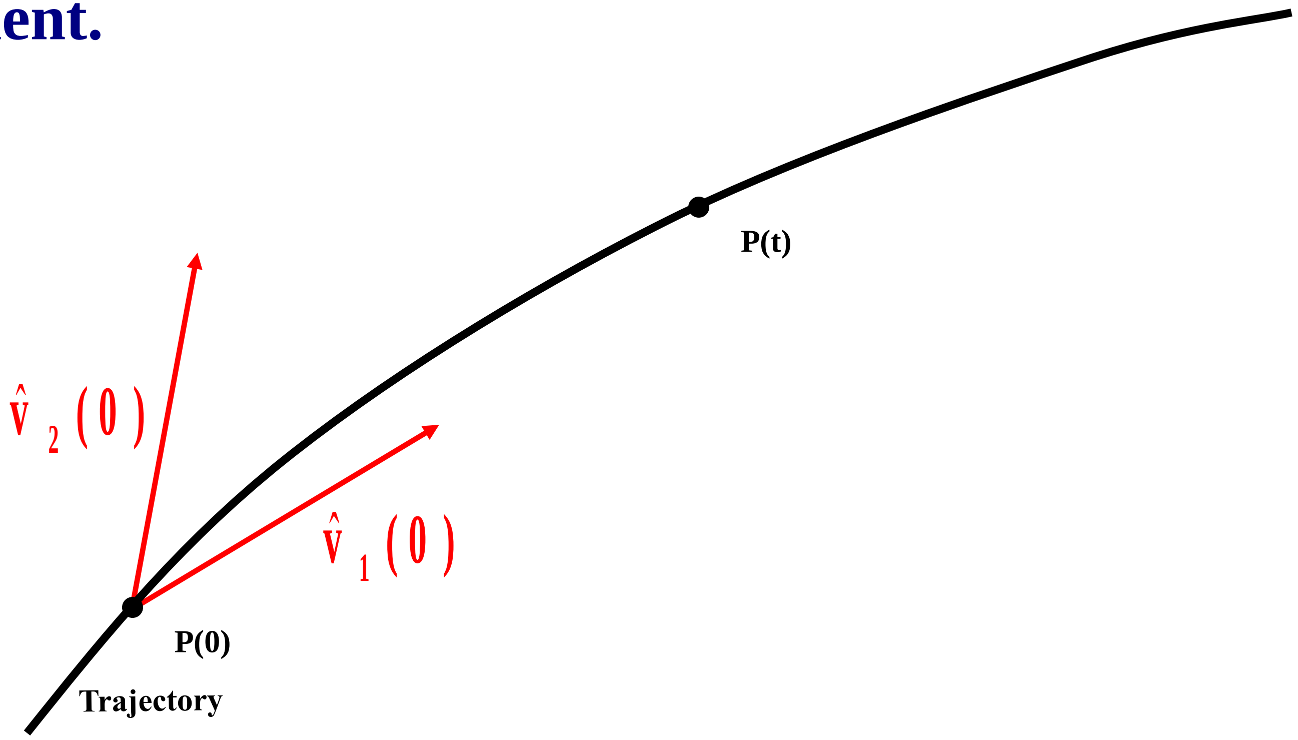

Behavior of the SALI for chaotic motion

For chaotic orbits the two initially different deviation vectors tend to coincide with the direction defined by the maximum Lyapunov exponent.

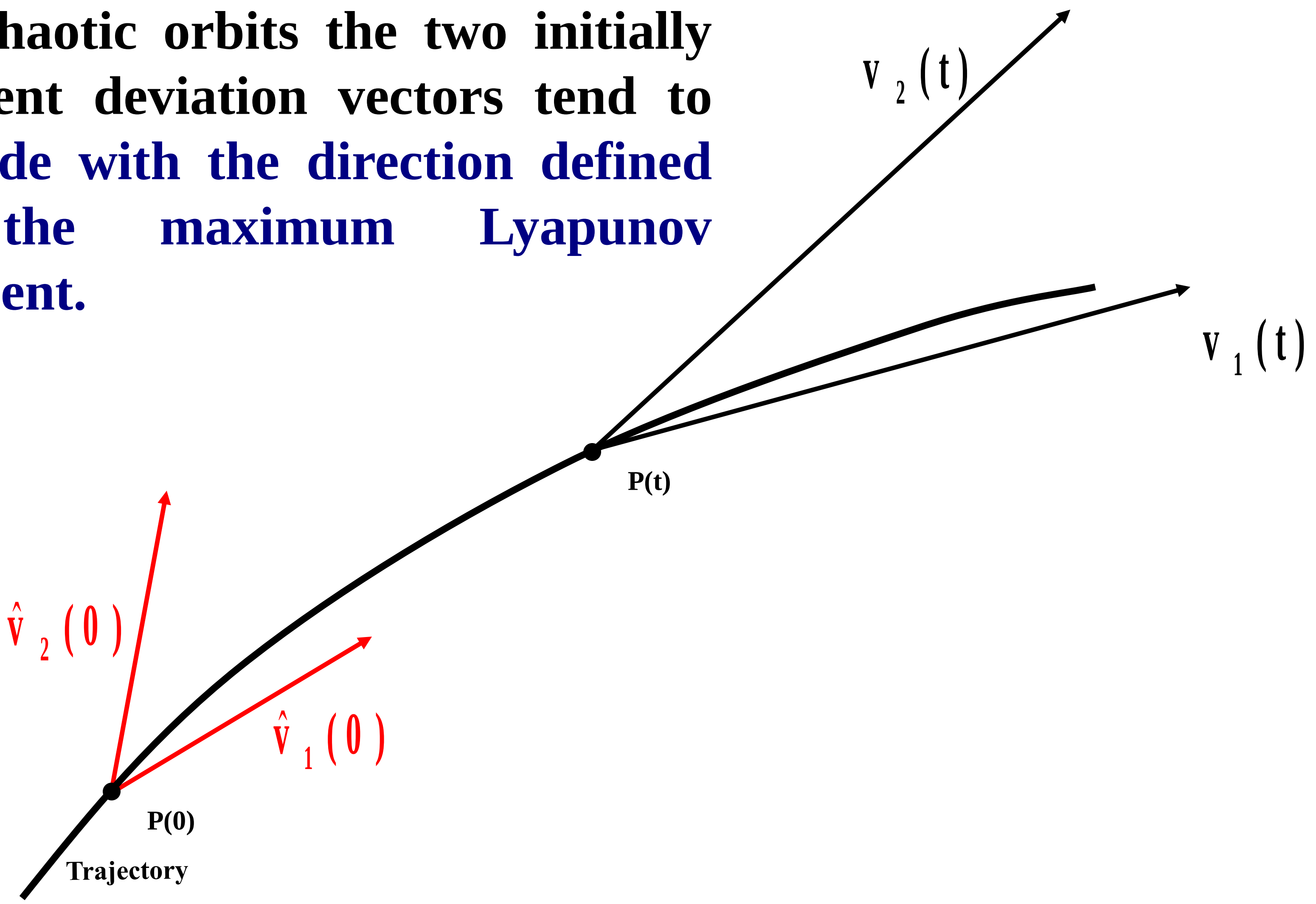

Behavior of the SALI for chaotic motion

For chaotic orbits the two initially different deviation vectors tend to coincide with the direction defined by the maximum Lyapunov exponent.

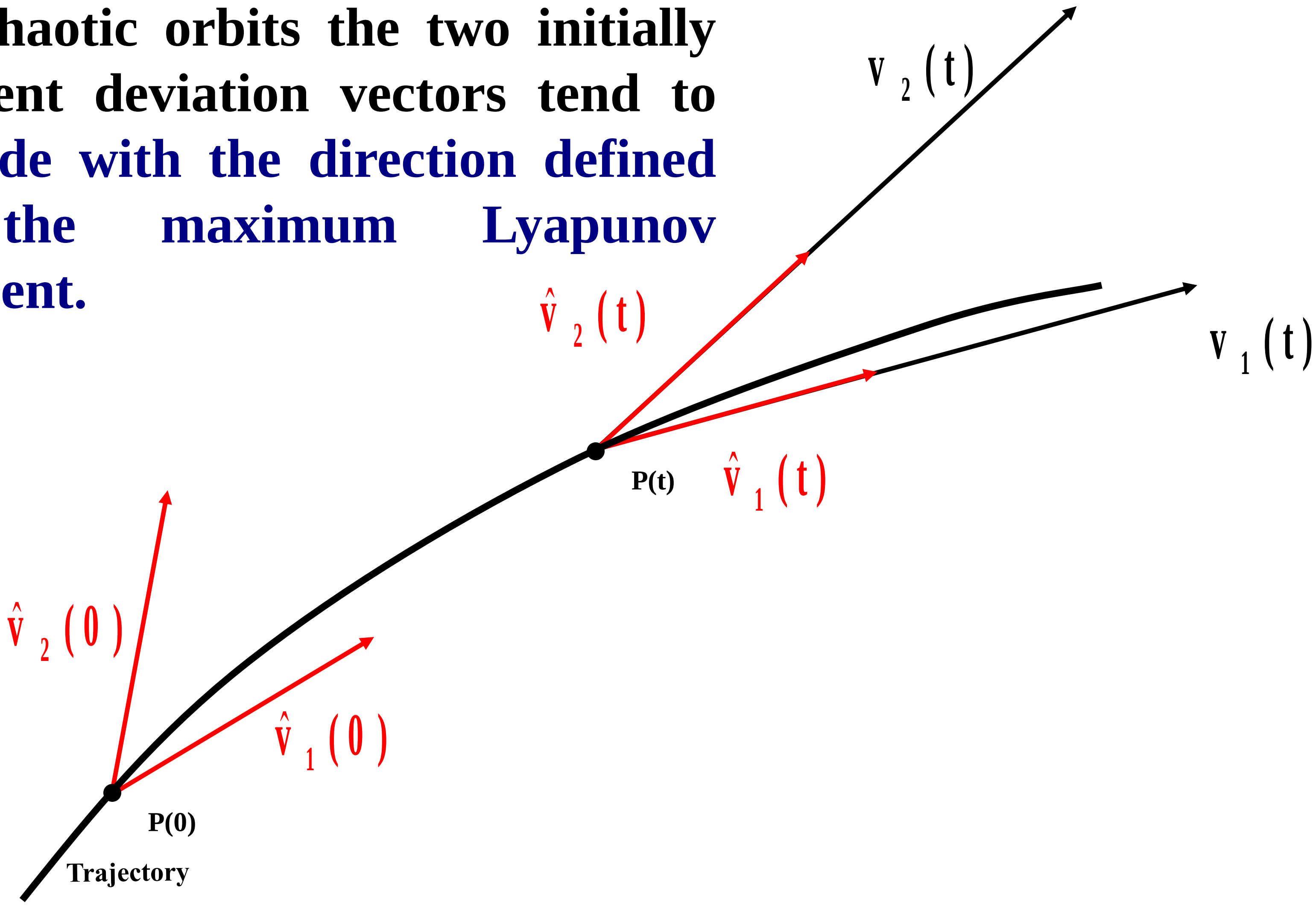

Behavior of the SALI for chaotic motion

For chaotic orbits the two initially different deviation vectors tend to coincide with the direction defined by the maximum Lyapunov exponent.

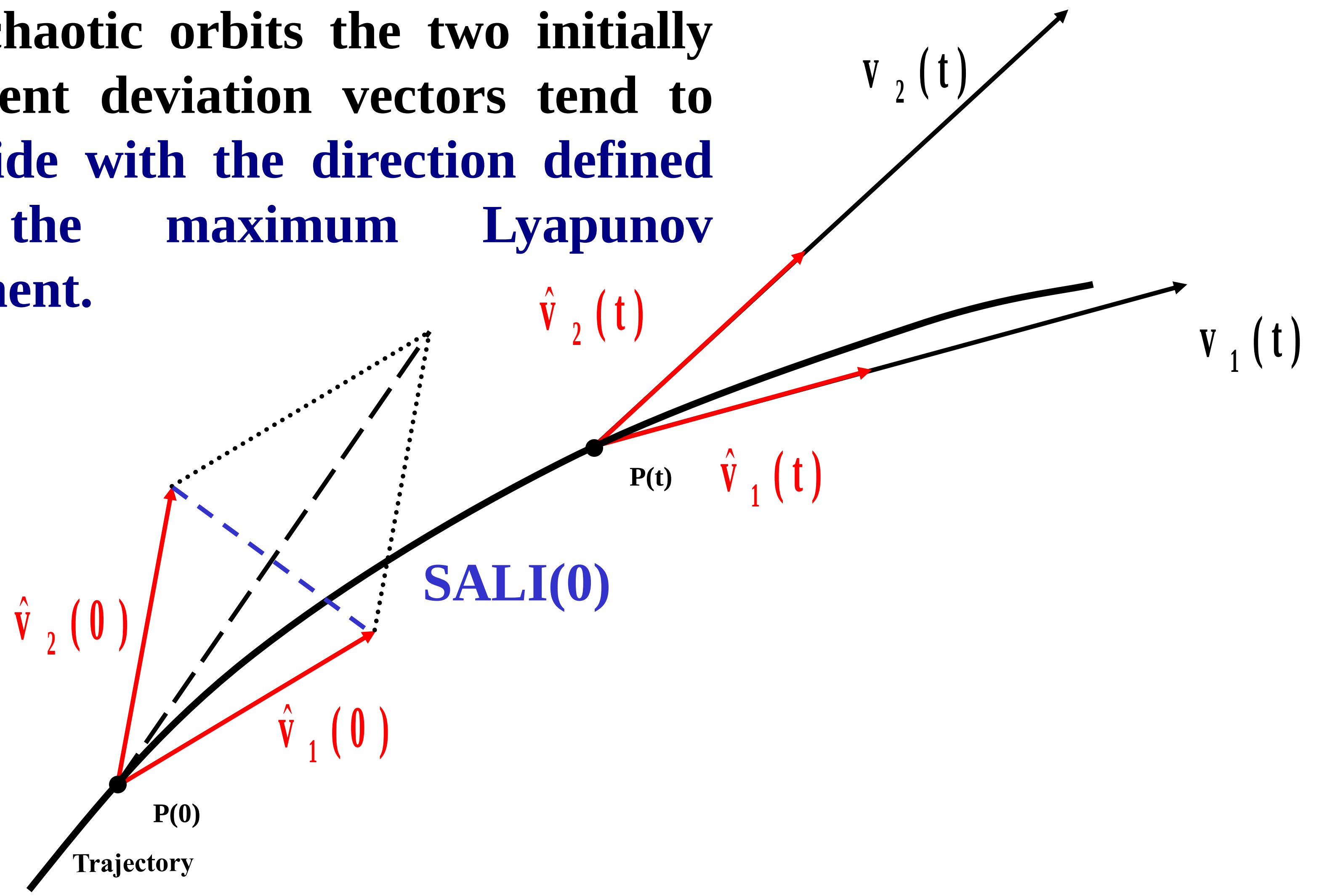

Behavior of the SALI for chaotic motion

For chaotic orbits the two initially different deviation vectors tend to coincide with the direction defined by the maximum Lyapunov exponent.

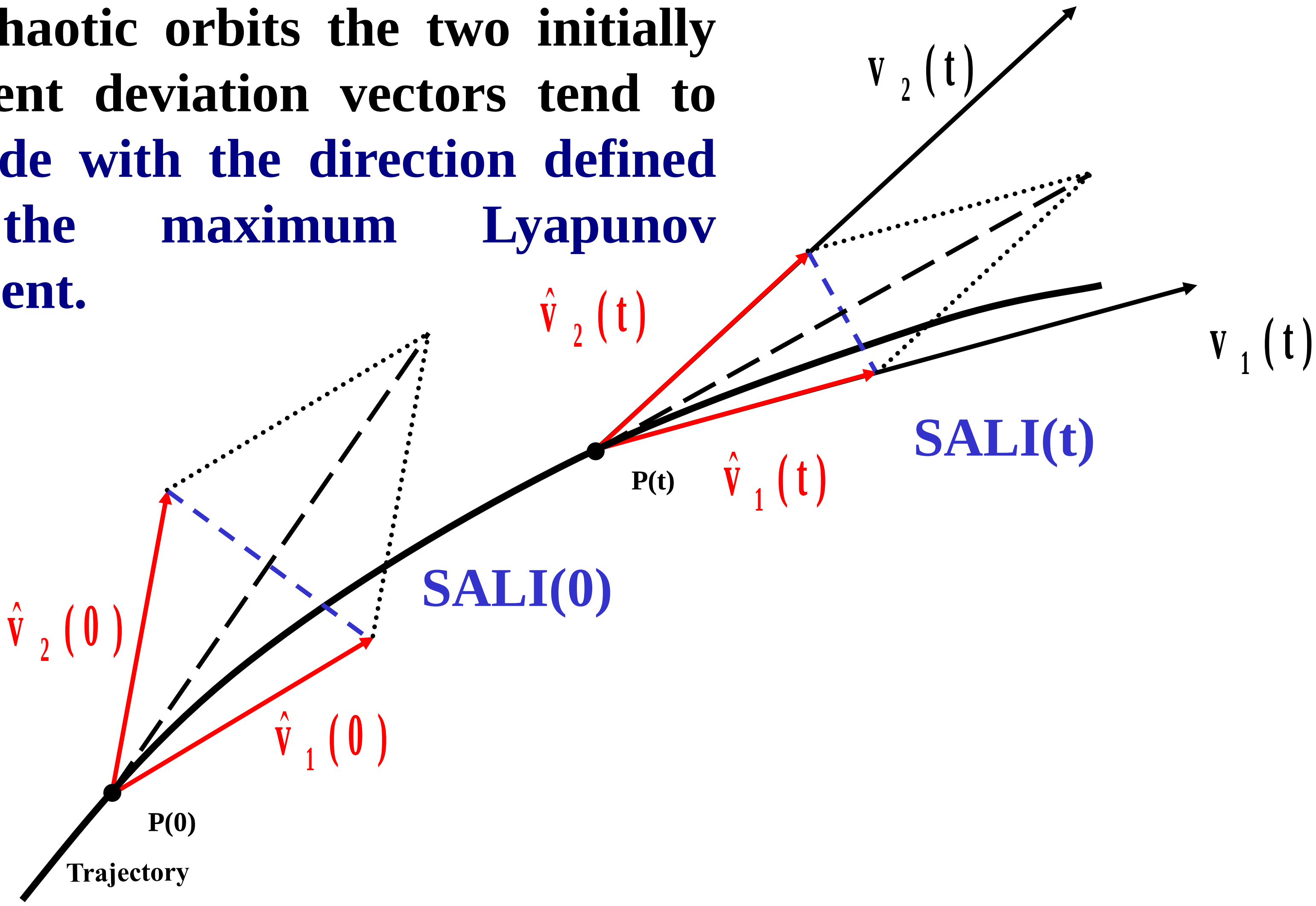

Behavior of the SALI for chaotic motion

We test the validity of the approximation SALI$\propto e^{-(\sigma_1-\sigma_2)t}$ (Ch.S., Antonopoulos, Bountis, Vrahatis, 2004, J. Phys. A) for a chaotic orbit of the 3D Hamiltonian

$$H = \sum_{i=1}^{3} \frac{\omega_i}{2}(q_i^2 + p_i^2) + q_1^2 q_2 + q_1^2 q_3$$

with ω_1=1, ω_2=1.4142, ω_3=1.7321, H=0.09

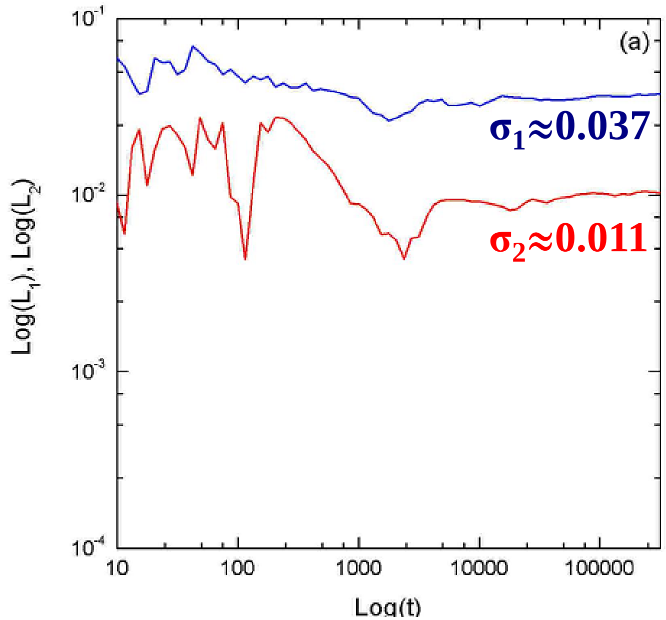

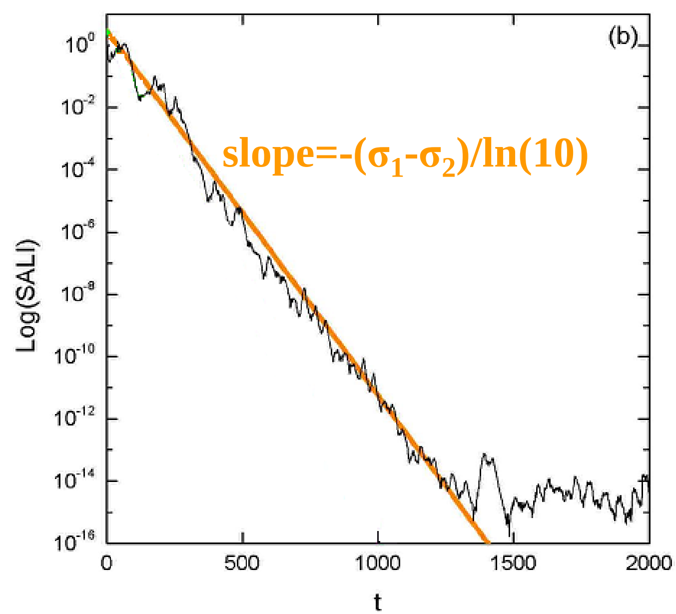

Behavior of the SALI for regular motion

Regular motion occurs on a torus and two different initial deviation vectors become tangent to the torus, generally having different directions.

Behavior of the SALI for regular motion

Regular motion occurs on a torus and two different initial deviation vectors become tangent to the torus, generally having different directions.

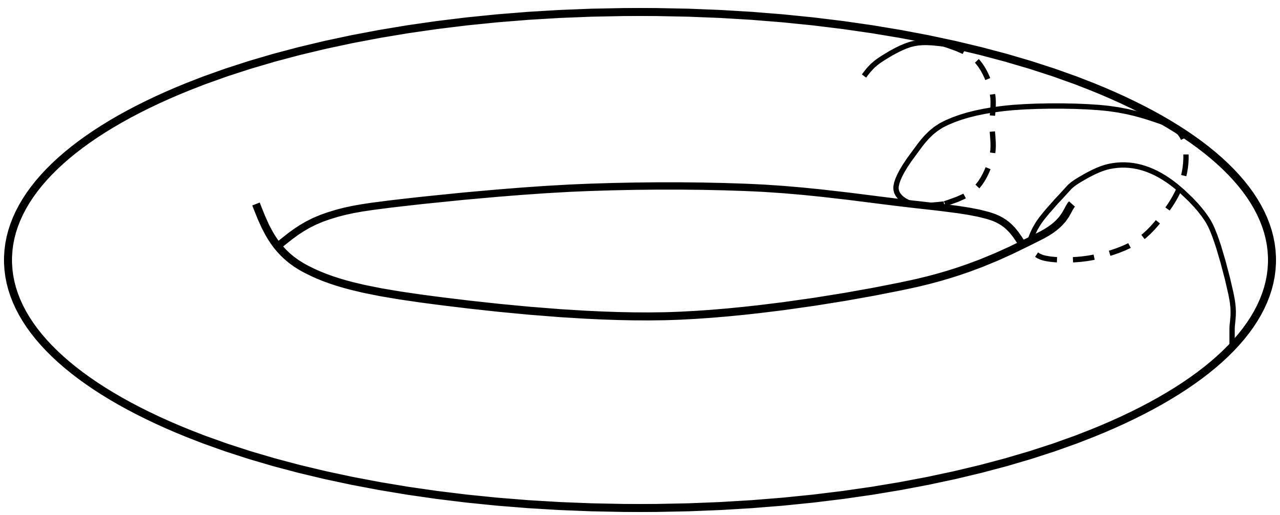

Behavior of the SALI for regular motion

Regular motion occurs on a torus and two different initial deviation vectors become tangent to the torus, generally having different directions.

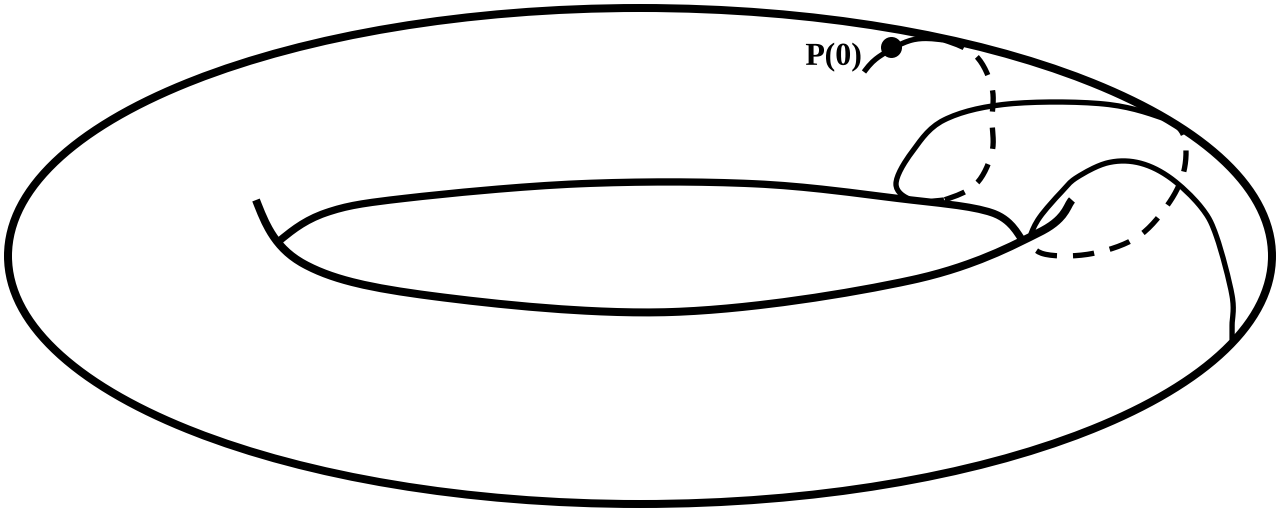

Behavior of the SALI for regular motion

Regular motion occurs on a torus and two different initial deviation vectors become tangent to the torus, generally having different directions.

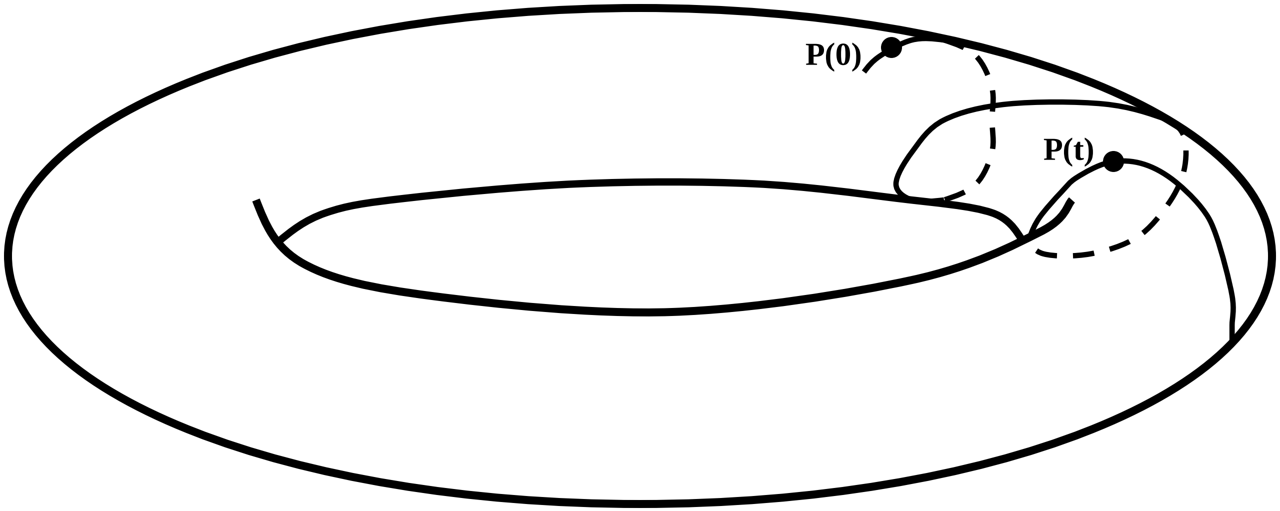

Behavior of the SALI for regular motion

Regular motion occurs on a torus and two different initial deviation vectors become tangent to the torus, generally having different directions.

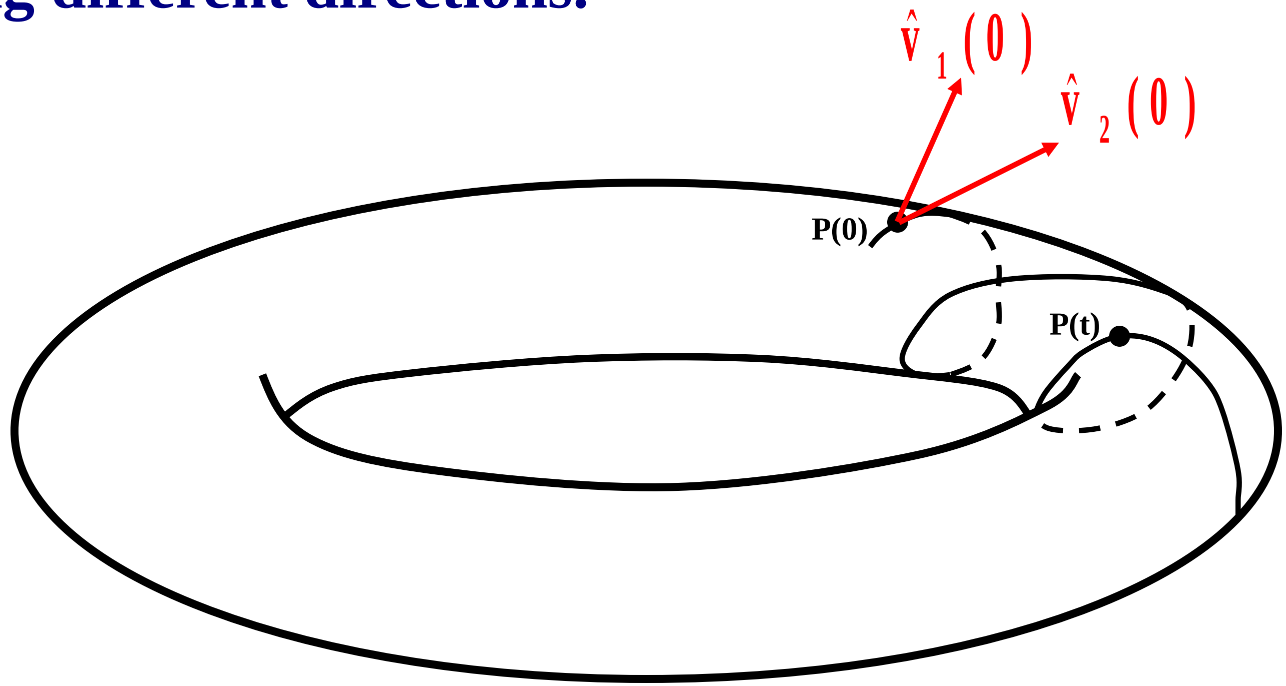

Behavior of the SALI for regular motion

Regular motion occurs on a torus and two different initial deviation vectors become tangent to the torus, generally having different directions.

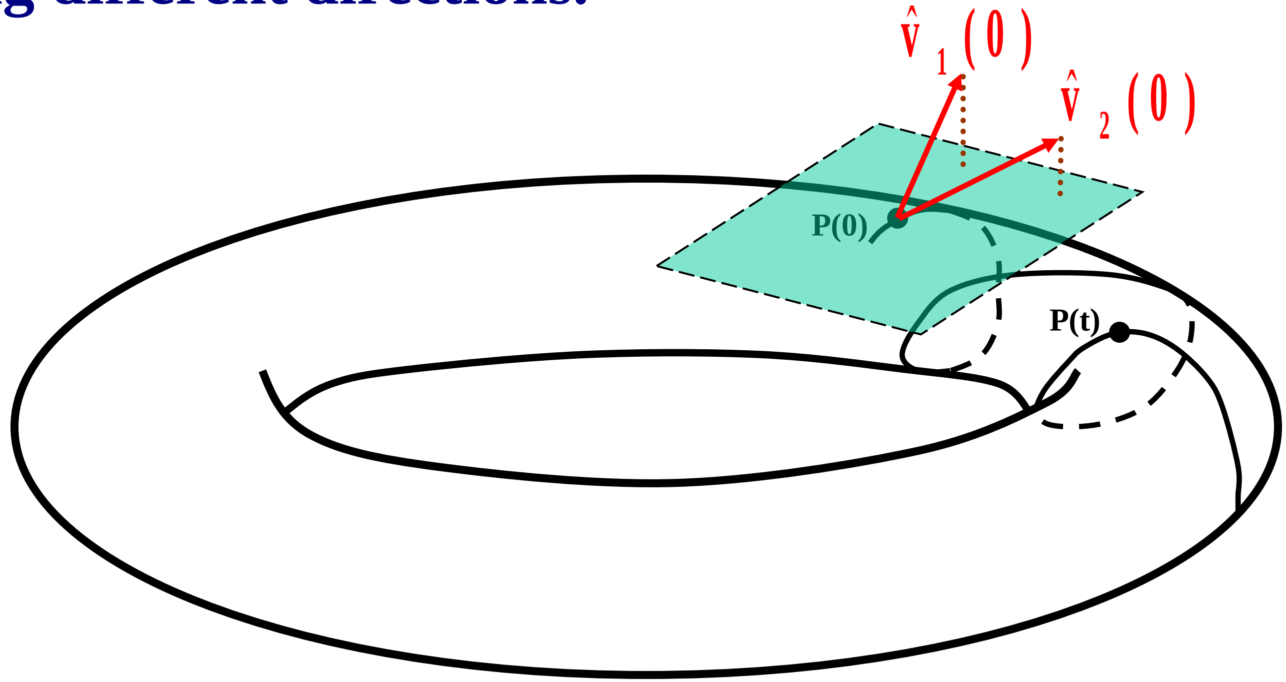

Behavior of the SALI for regular motion

Regular motion occurs on a torus and two different initial deviation vectors become tangent to the torus, generally having different directions.

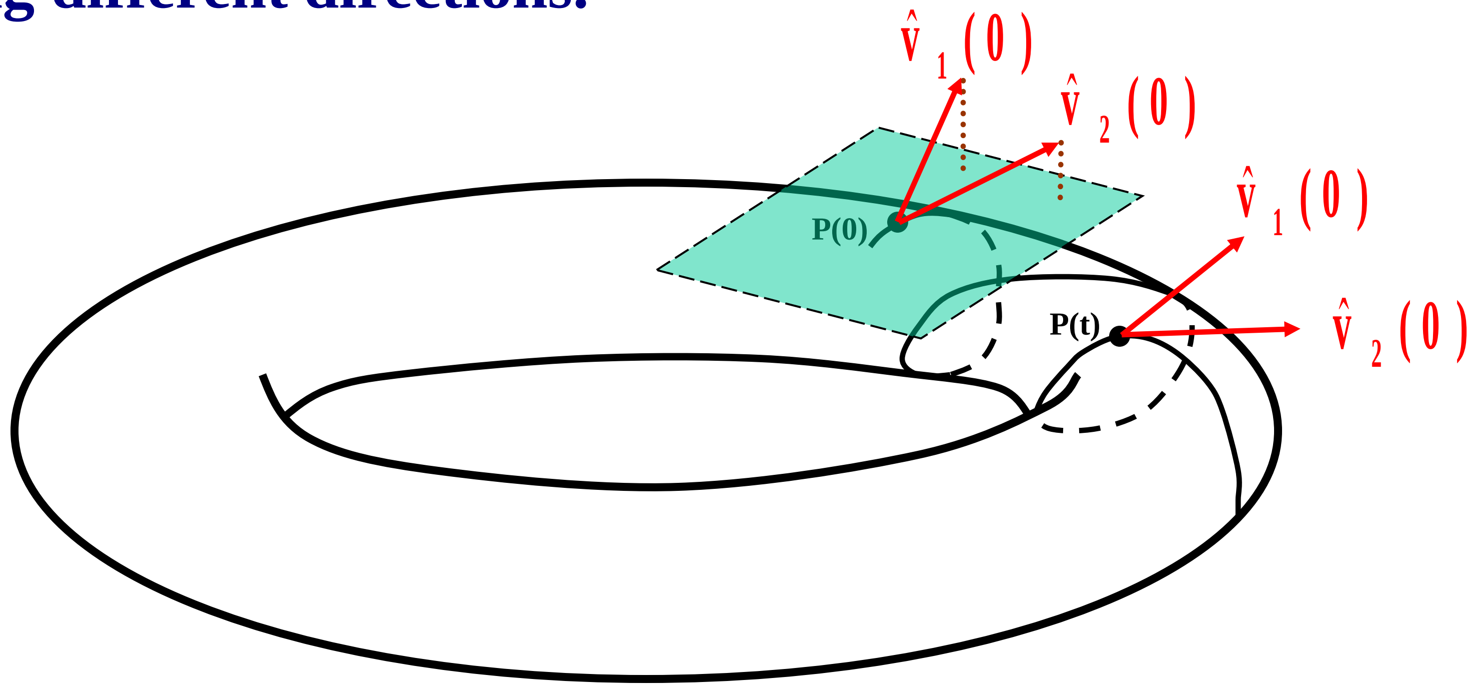

Behavior of the SALI for regular motion

Regular motion occurs on a torus and two different initial deviation vectors become tangent to the torus, generally having different directions.

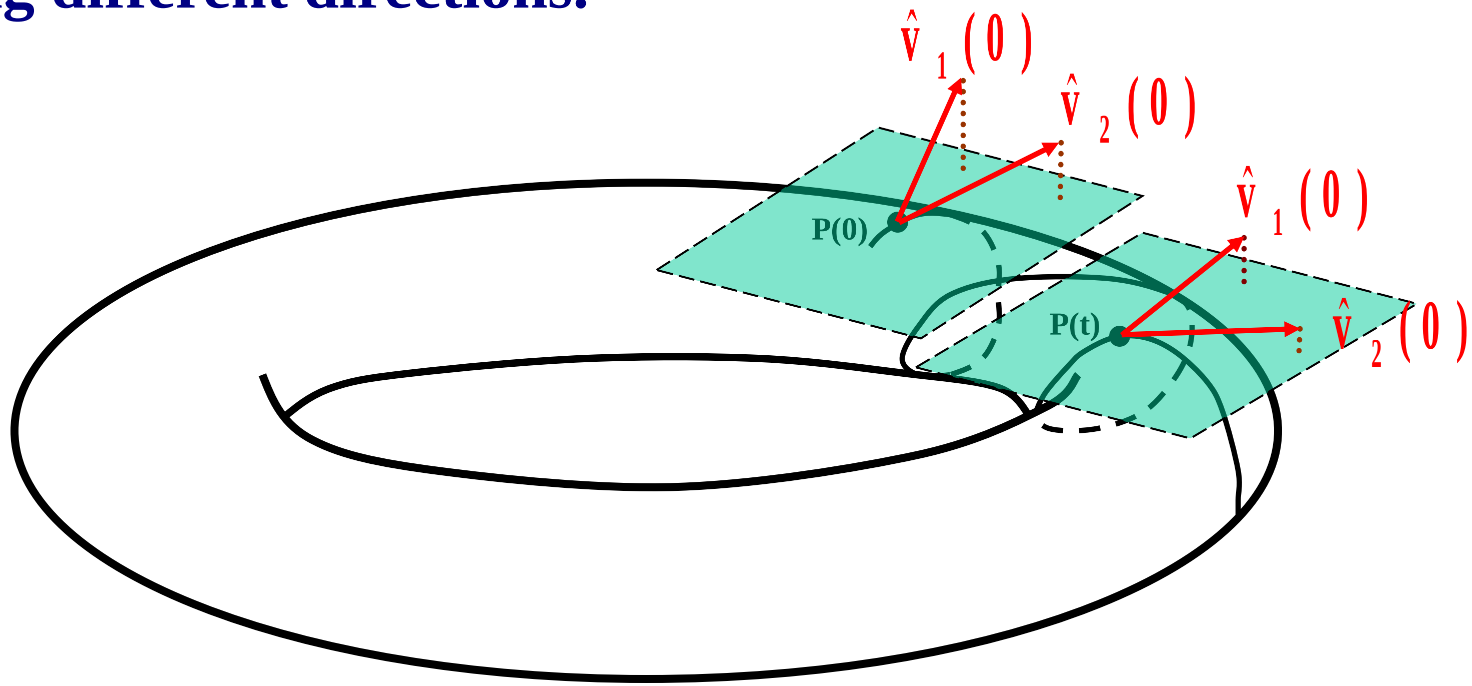

Applications – Hénon-Heiles system

As an example, we consider the 2D Hénon-Heiles system:

$$H_2 = \frac{1}{2}(p_x^2 + p_y^2) + \frac{1}{2}(x^2 + y^2) + x^2 y - \frac{1}{3}y^3$$

For E=1/8 we consider the orbits with initial conditions:
Regular orbit, $x=0$, $y=0.55$, $p_x=0.2417$, $p_y=0$
Chaotic orbit, $x=0$, $y=-0.016$, $p_x=0.49974$, $p_y=0$
Chaotic orbit, $x=0$, $y=-0.01344$, $p_x=0.49982$, $p_y=0$

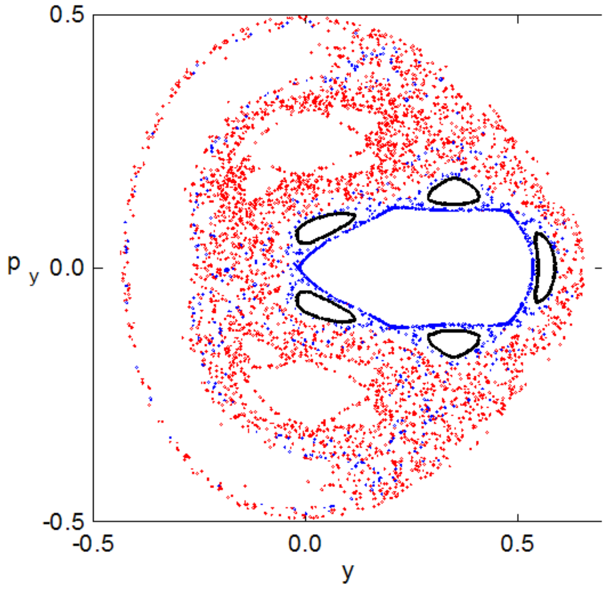

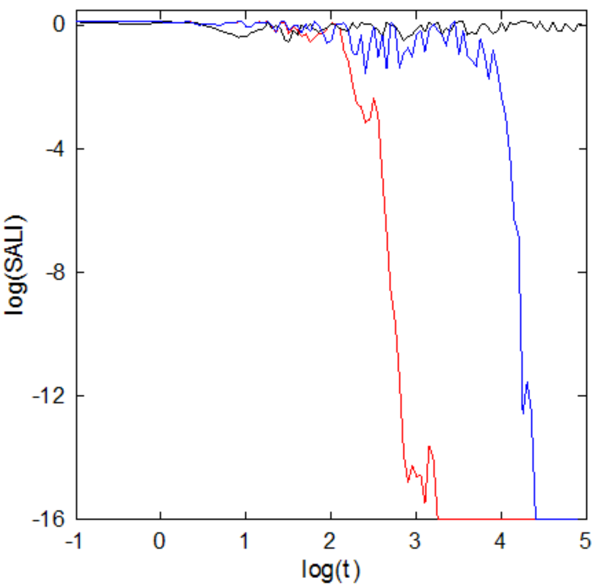

Applications – Hénon-Heiles system

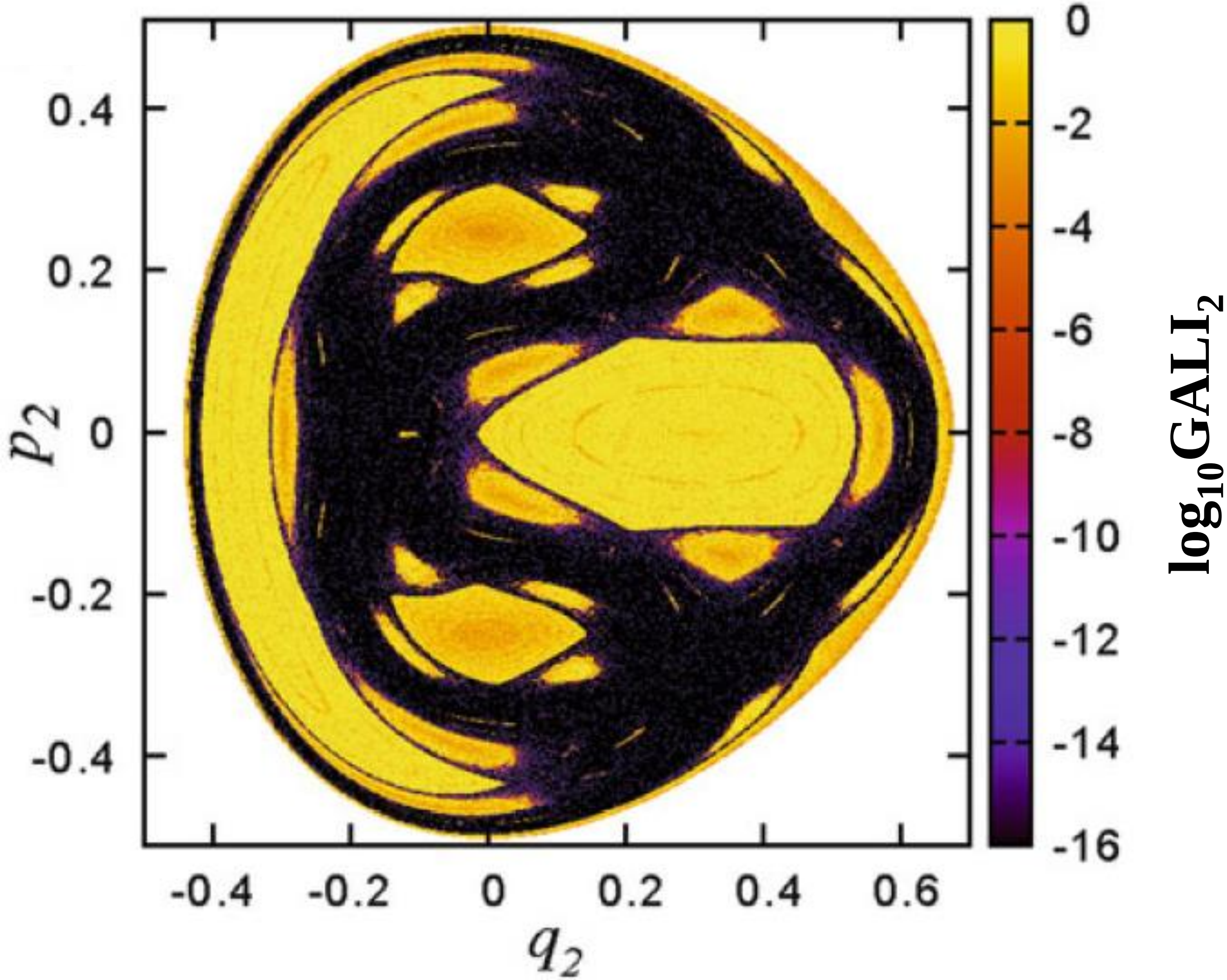

Applications – 4D map

$$\begin{aligned} x_1' &= x_1 + x_2 \\ x_2' &= x_2 - \nu \sin(x_1 + x_2) - \mu[1 - \cos(x_1 + x_2 + x_3 + x_4)] \\ x_3' &= x_3 + x_4 \\ x_4' &= x_4 - \kappa \sin(x_3 + x_4) - \mu[1 - \cos(x_1 + x_2 + x_3 + x_4)] \end{aligned} \quad (\text{mod } 2\pi)$$

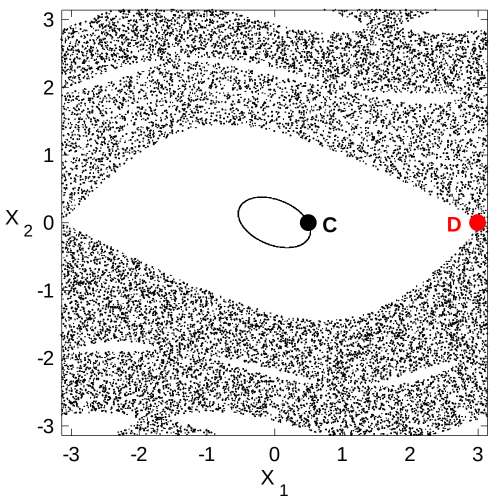

For ν=0.5, κ=0.1, μ=0.1 we consider the orbits:

regular orbit C *with initial conditions x_1=0.5, x_2=0, x_3=0.5, x_4=0.*

chaotic orbit D *with initial conditions x_1=3, x_2=0, x_3=0.5, x_4=0.*

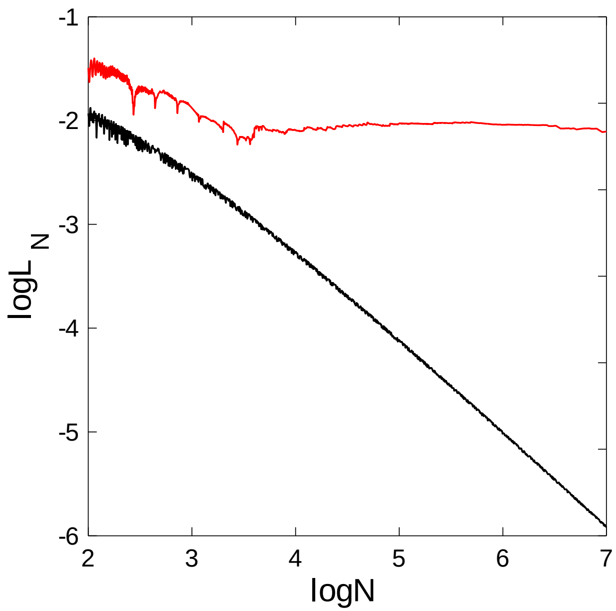

Applications – 4D map

$$\begin{aligned} x_1' &= x_1 + x_2 \\ x_2' &= x_2 - \nu \sin(x_1 + x_2) - \mu[1 - \cos(x_1 + x_2 + x_3 + x_4)] \\ x_3' &= x_3 + x_4 \\ x_4' &= x_4 - \kappa \sin(x_3 + x_4) - \mu[1 - \cos(x_1 + x_2 + x_3 + x_4)] \end{aligned} \quad (\text{mod } 2\pi)$$

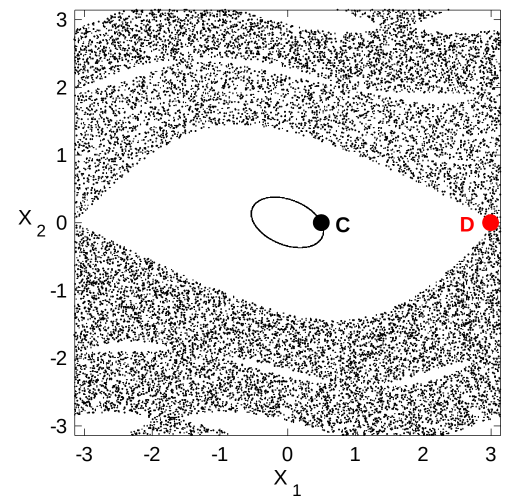

For ν=0.5, κ=0.1, μ=0.1 we consider the orbits:

regular orbit C *with initial conditions* $x_1=0.5$, $x_2=0$, $x_3=0.5$, $x_4=0$.

chaotic orbit D *with initial conditions* $x_1=3$, $x_2=0$, $x_3=0.5$, $x_4=0$.

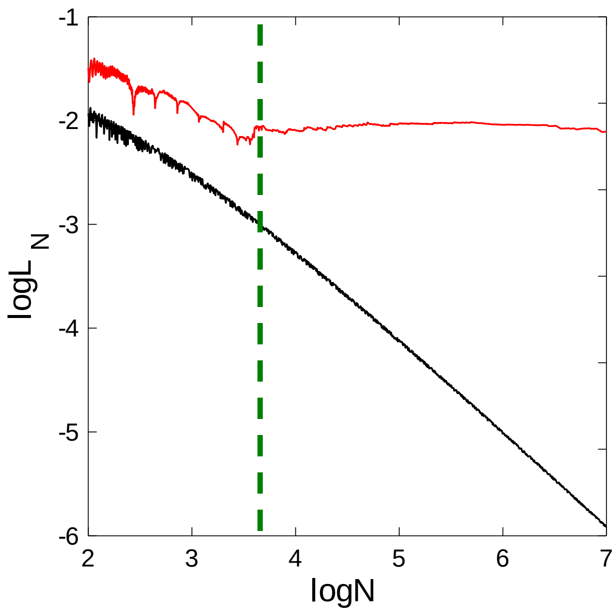

Applications – 4D map

$$
\begin{aligned}
x_1' &= x_1 + x_2 \\
x_2' &= x_2 - \nu \sin(x_1 + x_2) - \mu[1 - \cos(x_1 + x_2 + x_3 + x_4)] \\
x_3' &= x_3 + x_4 \\
x_4' &= x_4 - \kappa \sin(x_3 + x_4) - \mu[1 - \cos(x_1 + x_2 + x_3 + x_4)]
\end{aligned}
\quad (\text{mod } 2\pi)
$$

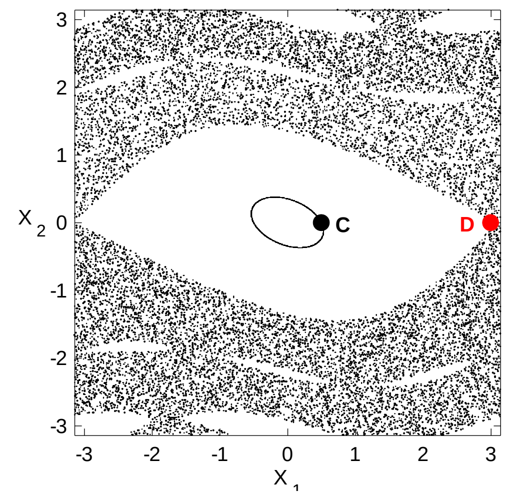

For ν=0.5, κ=0.1, μ=0.1 we consider the orbits:

regular orbit C *with initial conditions* $x_1=0.5$, $x_2=0$, $x_3=0.5$, $x_4=0$.

chaotic orbit D *with initial conditions* $x_1=3$, $x_2=0$, $x_3=0.5$, $x_4=0$.

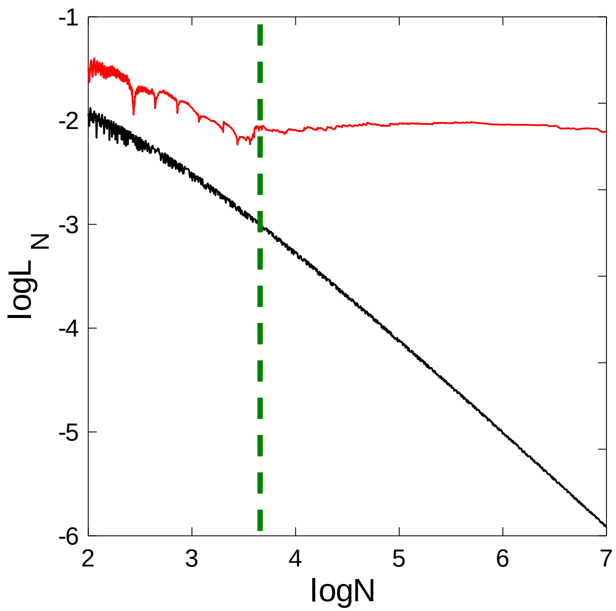

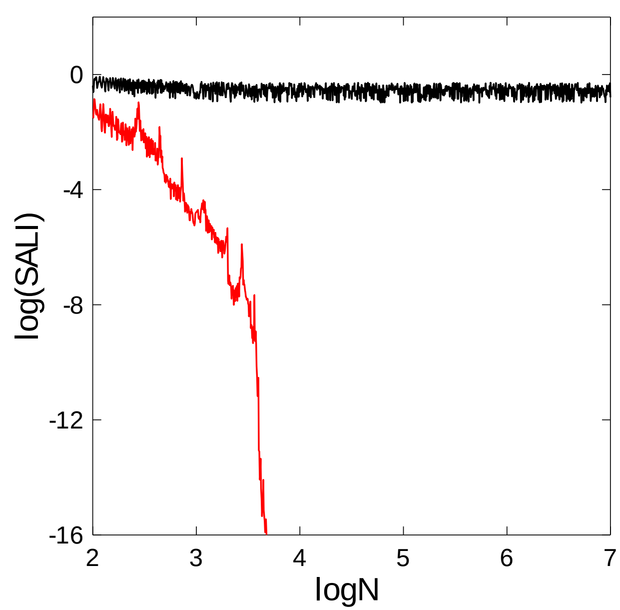

Applications – 4D map

$$\begin{aligned} x_1' &= x_1 + x_2 \\ x_2' &= x_2 - \nu \sin(x_1 + x_2) - \mu[1-\cos(x_1+x_2+x_3+x_4)] \\ x_3' &= x_3 + x_4 \\ x_4' &= x_4 - \kappa \sin(x_3 + x_4) - \mu[1-\cos(x_1+x_2+x_3+x_4)] \end{aligned} \quad (\text{mod } 2\pi)$$

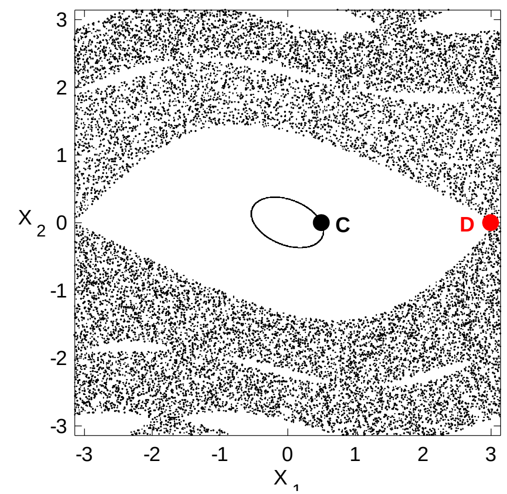

For ν=0.5, κ=0.1, μ=0.1 we consider the orbits:

regular orbit C *with initial conditions* $x_1=0.5$, $x_2=0$, $x_3=0.5$, $x_4=0$.

chaotic orbit D *with initial conditions* $x_1=3$, $x_2=0$, $x_3=0.5$, $x_4=0$.

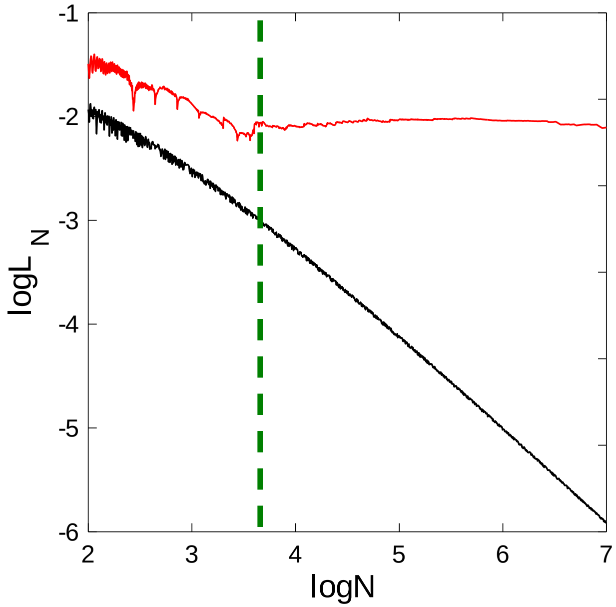

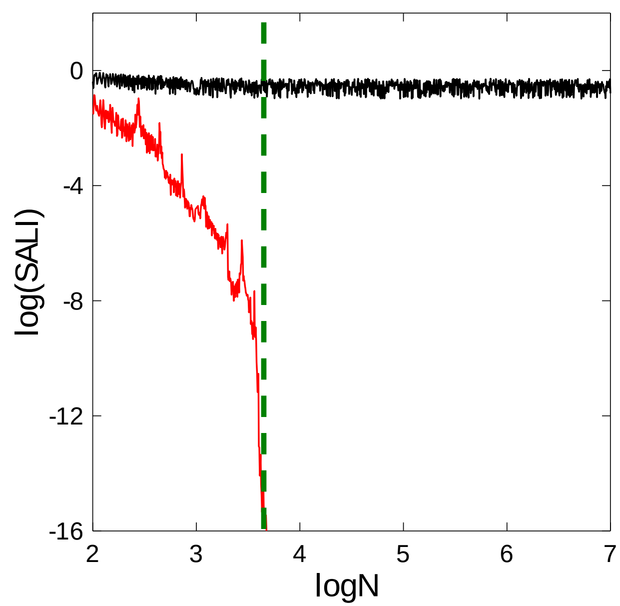

The
Generalized ALignment Indices
(GALIs)
method

Definition of the Generalized Alignment Index (GALI)

SALI effectively measures the ‘area’ of the parallelogram formed by the two deviation vectors.

Definition of the Generalized Alignment Index (GALI)

SALI effectively measures the 'area' of the parallelogram formed by the two deviation vectors.

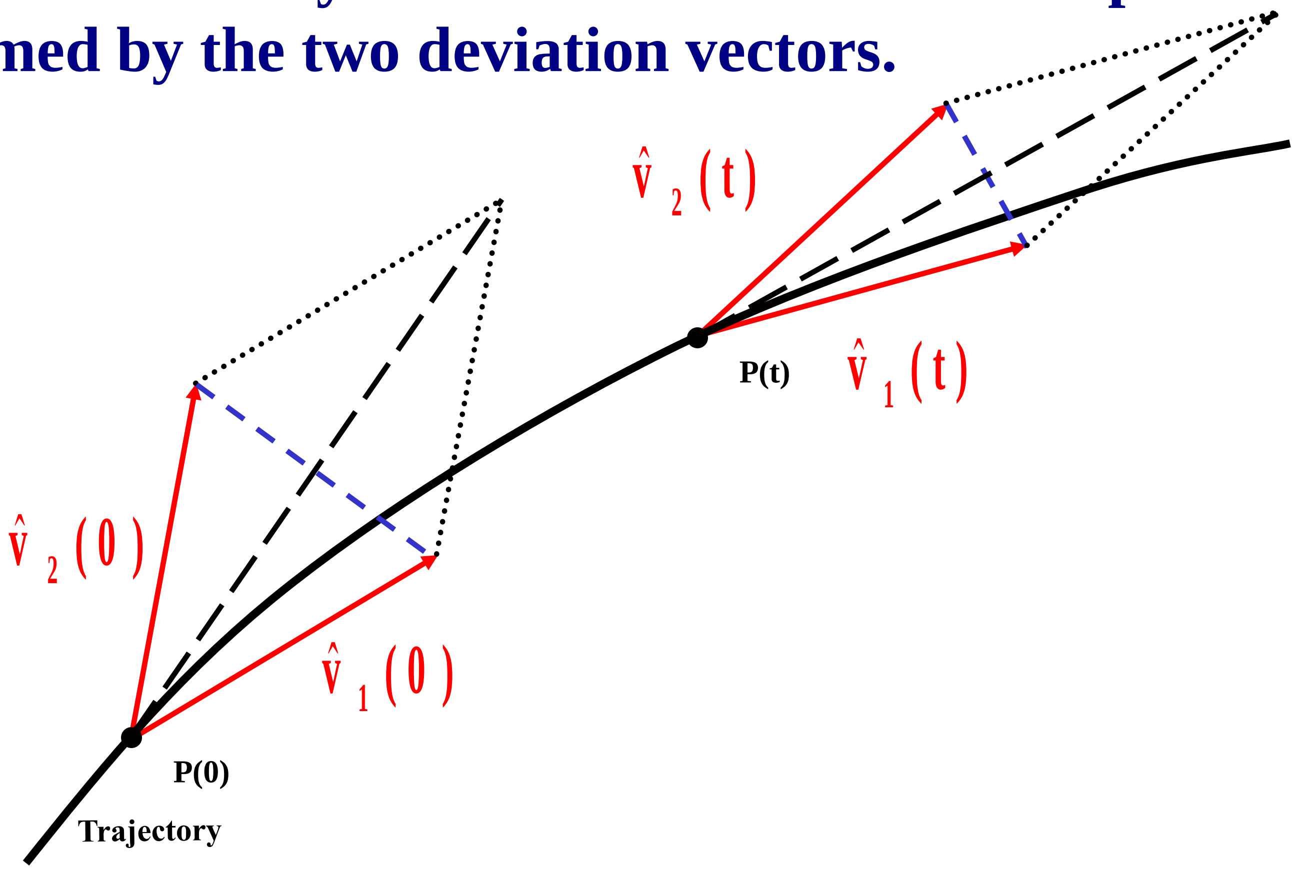

Definition of the Generalized Alignment Index (GALI)

SALI effectively measures the 'area' of the parallelogram formed by the two deviation vectors.

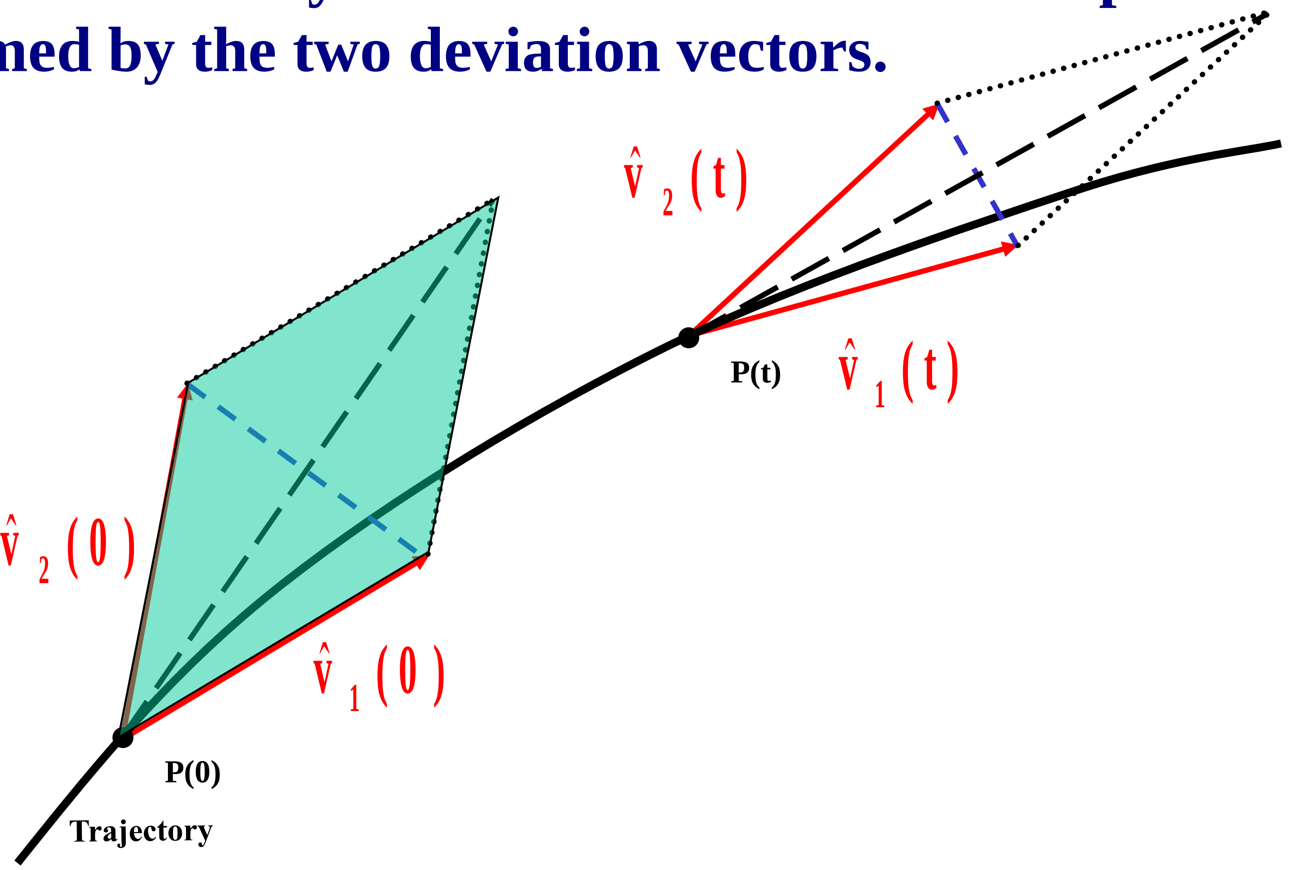

Definition of the Generalized Alignment Index (GALI)

SALI effectively measures the 'area' of the parallelogram formed by the two deviation vectors.

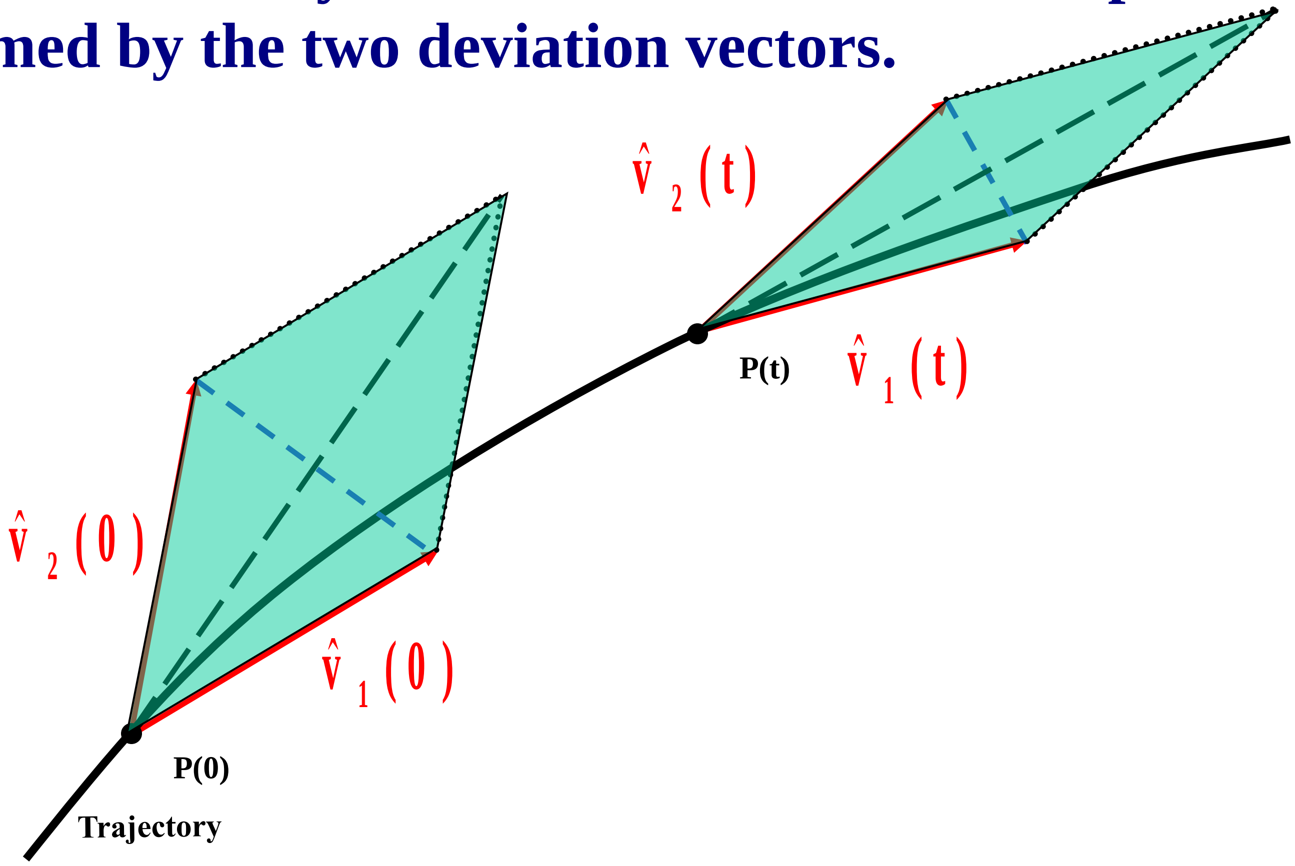

Definition of the Generalized Alignment Index (GALI)

SALI effectively measures the ‘area’ of the parallelogram formed by the two deviation vectors.

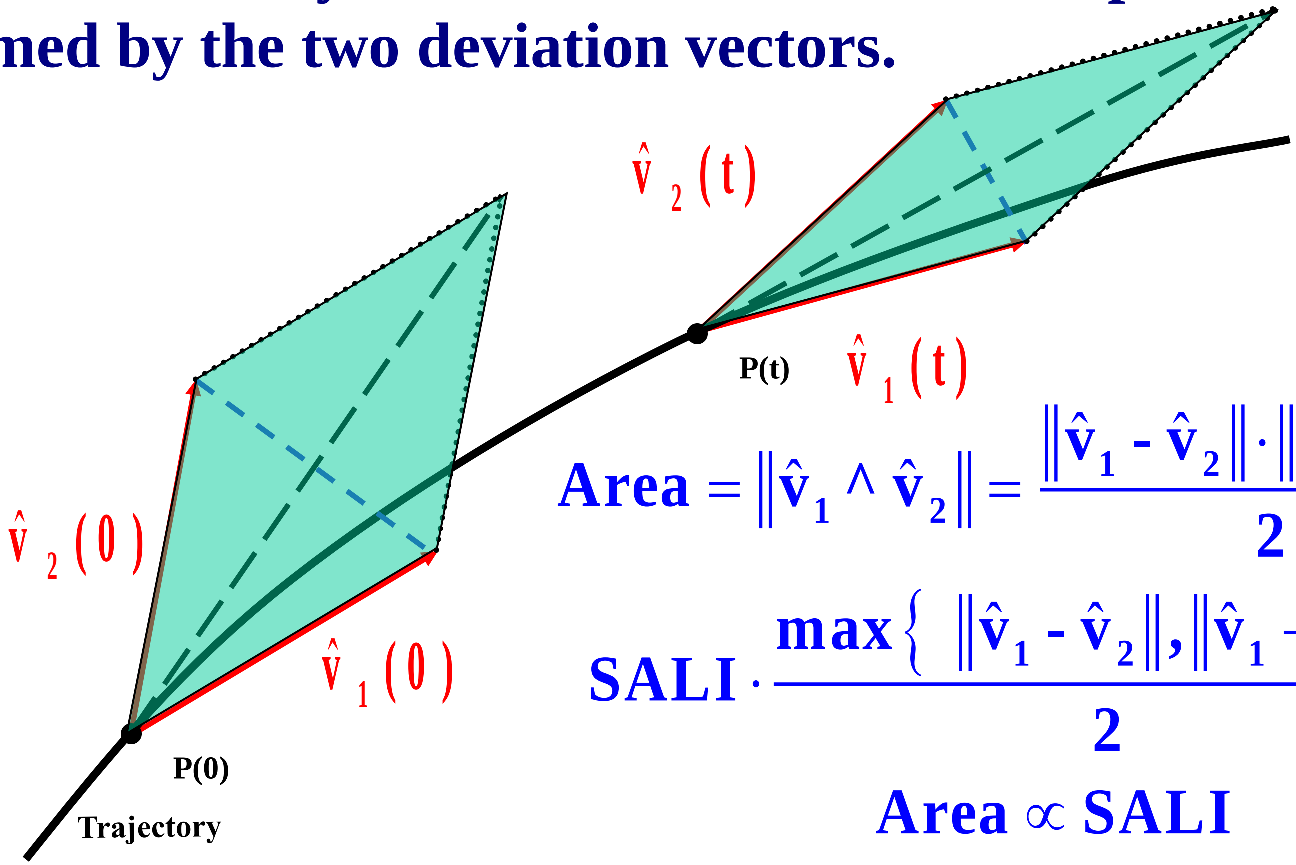

$$\mathbf{Area} = \left\| \hat{\mathbf{v}}_1 \wedge \hat{\mathbf{v}}_2 \right\| = \frac{\left\| \hat{\mathbf{v}}_1 - \hat{\mathbf{v}}_2 \right\| \cdot \left\| \hat{\mathbf{v}}_1 + \hat{\mathbf{v}}_2 \right\|}{2} =$$

$$\mathbf{SALI} \cdot \frac{\mathbf{max}\left\{ \left\| \hat{\mathbf{v}}_1 - \hat{\mathbf{v}}_2 \right\|, \left\| \hat{\mathbf{v}}_1 + \hat{\mathbf{v}}_2 \right\| \right\}}{2} \Rightarrow$$

$$\mathbf{Area} \propto \mathbf{SALI}$$

Definition of the GALI

In the case of an N degree of freedom Hamiltonian system or a 2N symplectic map we follow the evolution of

k deviation vectors with 2≤k≤2N,

and define (Ch.S., Bountis, Antonopoulos, 2007, Physica D) the Generalized Alignment Index (GALI) of order k :

$$GALI_k(t) = \left\| \hat{v}_1(t) \wedge \hat{v}_2(t) \wedge \ldots \wedge \hat{v}_k(t) \right\|$$

where

$$\hat{v}_1(t) = \frac{v_1(t)}{\left\| v_1(t) \right\|}$$

Behavior of the $GALI_k$ for chaotic motion

$GALI_k$ ($2 \leq k \leq 2N$) tends exponentially to zero with exponents that involve the values of the first k largest Lyapunov exponents $\sigma_1, \sigma_2, \ldots, \sigma_k$:

$$GALI_k(t) \propto e^{-[(\sigma_1-\sigma_2)+(\sigma_1-\sigma_3)+\ldots+(\sigma_1-\sigma_k)]t}$$

The above relation is valid even if some Lyapunov exponents are equal, or very close to each other.

Behavior of the $\mathbf{GALI_k}$ for chaotic motion

N particles Fermi-Pasta-Ulam (FPU) system:

$$H = \frac{1}{2}\sum_{i=1}^{N} p_i^2 + \sum_{i=0}^{N}\left[\frac{1}{2}\left(q_{i+1} - q_i\right)^2 + \frac{\beta}{4}\left(q_{i+1} - q_i\right)^4\right]$$

with fixed boundary conditions, N=8 and β=1.5.

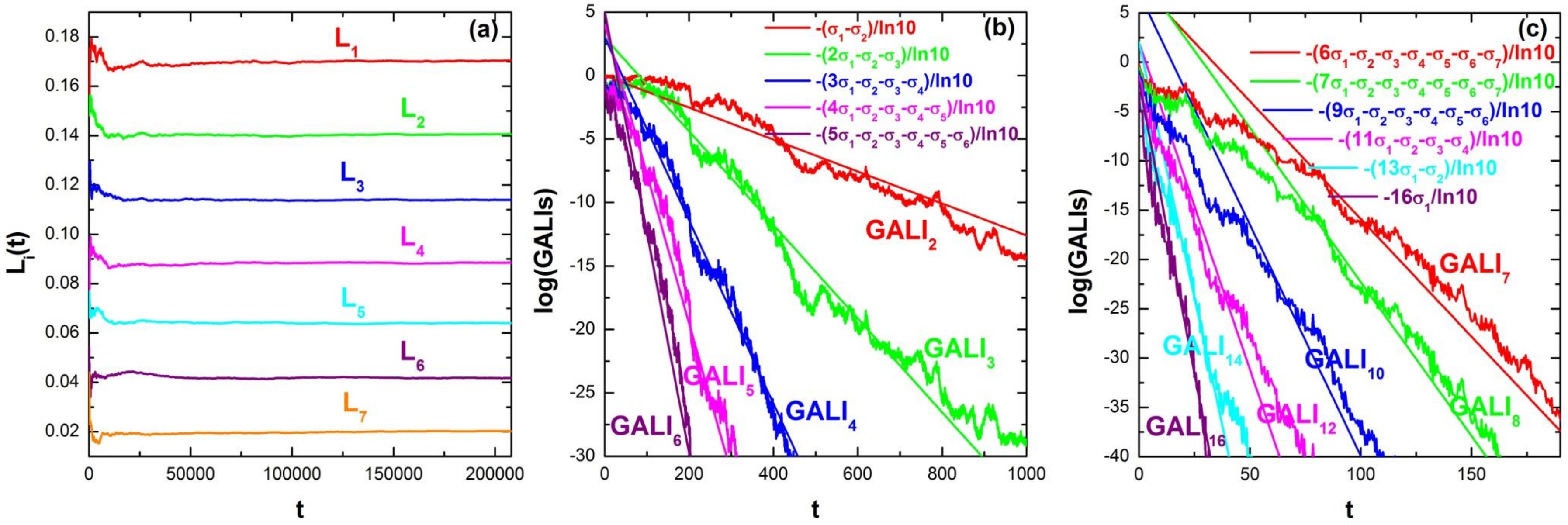

Behavior of the GALI$_k$ for regular motion

If the motion occurs on an s-dimensional torus with s≤N then the behavior of GALI$_k$ is given by (Ch.S., Bountis, Antonopoulos, 2008, Eur. Phys. J. Sp. Top.):

$$\mathrm{GALI}_k(t) \propto \begin{cases} \text{constant} & \text{if} \quad 2 \le k \le s \\ \dfrac{1}{t^{k-s}} & \text{if} \quad s < k \le 2N - s \\ \dfrac{1}{t^{2(k-N)}} & \text{if} \quad 2N - s < k \le 2N \end{cases}$$

while in the common case with s=N we have :

$$\mathrm{GALI}_k(t) \propto \begin{cases} \text{constant} & \text{if} \quad 2 \le k \le N \\ \dfrac{1}{t^{2(k-N)}} & \text{if} \quad N < k \le 2N \end{cases}$$

Behavior of the $GALI_k$ for regular motion

N=8 FPU system

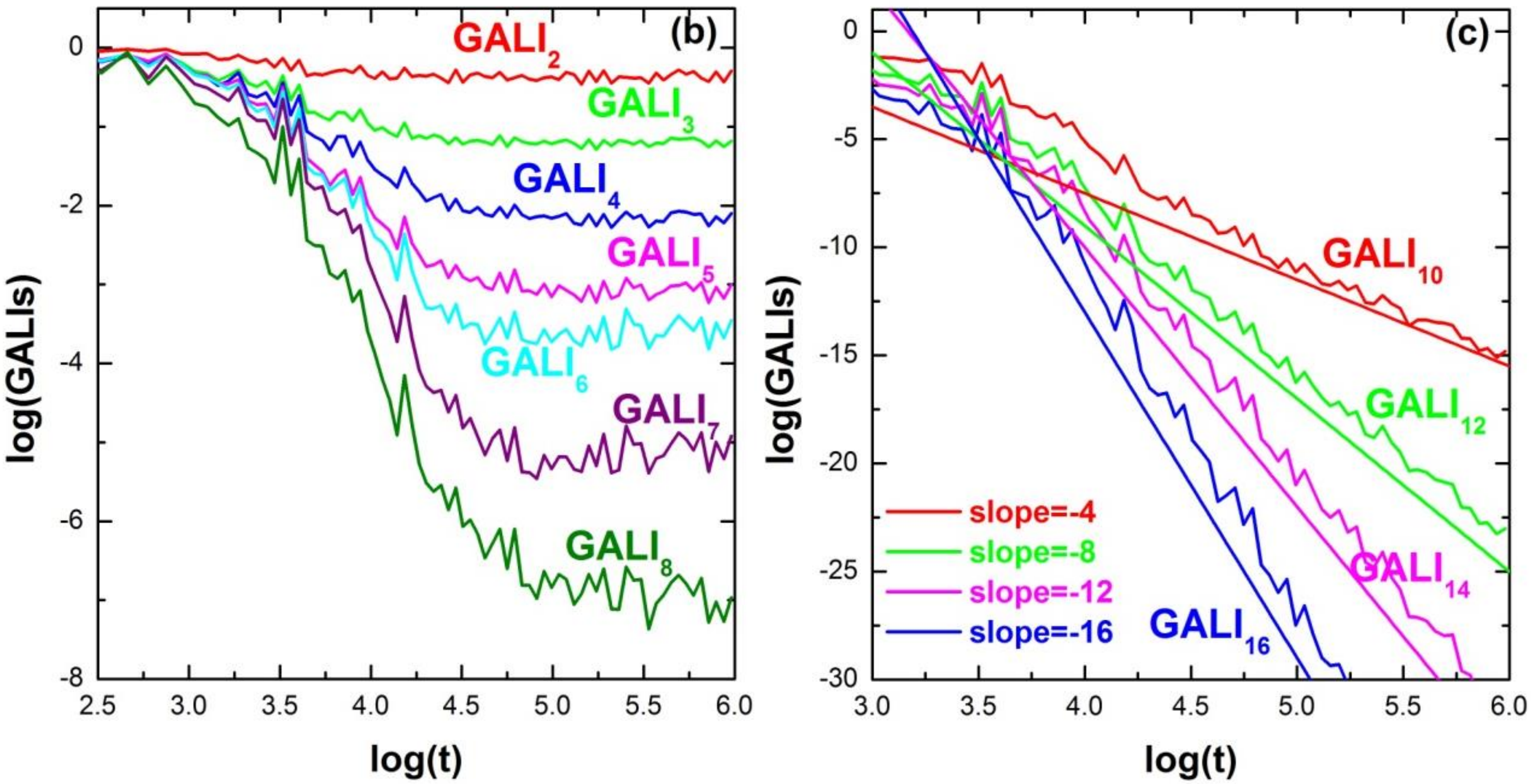

A time-dependent Hamiltonian system

Barred galaxies

NGC 1433

NGC 2217

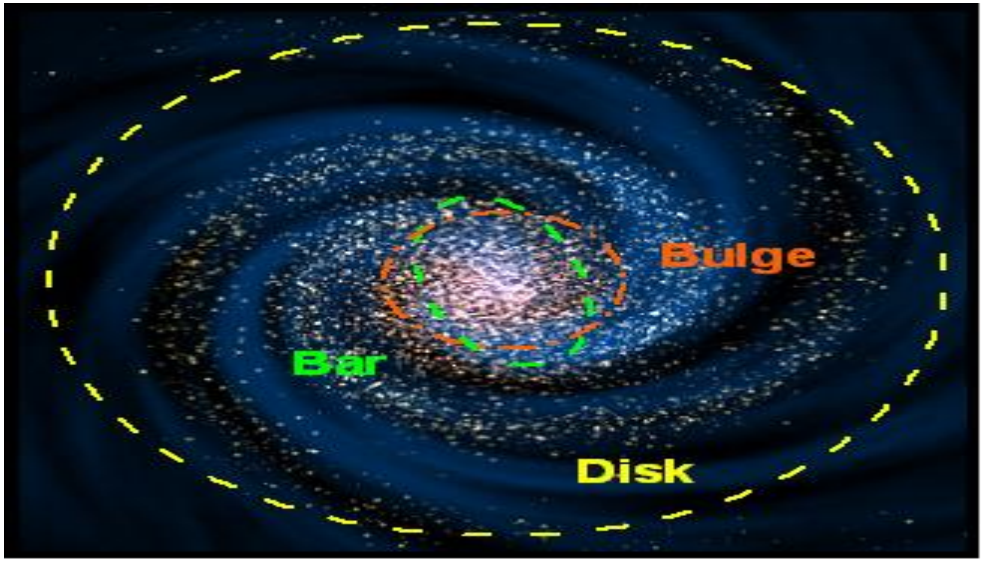

Barred galaxy model

The 3D bar rotates around its short *z*-axis (*x*: long axis and *y*: intermediate). The Hamiltonian that describes the motion for this model is:

$$H = \frac{1}{2}(p_x^2 + p_y^2 + p_z^2) + V(x,y,z) - \Omega_b(xp_y - yp_x) \equiv Energy$$

This model consists of the superposition of potentials describing an axisymmetric part and a bar component of the galaxy (Manos, Bountis, Ch.S., 2013, J. Phys. A).

a) Axisymmetric component:

i) Plummer sphere:

$$V_{sphere}(x,y,z) = -\frac{GM_S}{\sqrt{x^2 + y^2 + z^2 + \varepsilon_s^2}}$$

ii) Miyamoto–Nagai disc:

$$V_{disc}(x,y,z) = -\frac{GM_D}{\sqrt{x^2 + y^2 + (A + \sqrt{B^2 + z^2})^2}}$$

b) Bar component: $V_{bar}(x,y,z) = -\pi Gabc \frac{\rho_c}{n+1}\int_{\lambda}^{\infty} \frac{du}{\Delta(u)}(1 - m^2(u))^{n+1},$

(Ferrers bar)

$$\rho_c = \frac{105}{32\pi}\frac{GM_B}{abc}$$

$where\ m^2(u) = \frac{x^2}{a^2+u} + \frac{y^2}{b^2+u} + \frac{z^2}{c^2+u},\ \Delta^2(u) = (a^2+u)(b^2+u)(c^2+u),$

n: positive integer ($n = 2$ for our model), λ: the unique positive solution of $m^2(\lambda) = 1$

Its density is:

$$\rho = \begin{cases} \rho_c(1-m^2)^n, & \text{for } m \le 1 \\ 0, & \text{for } m > 1 \end{cases},\ \text{where } m^2 = \frac{x^2}{a^2} + \frac{y^2}{b^2} + \frac{z^2}{c^2},\ a > b > c \text{ and } n = 2.$$

Time-dependent barred galaxy model

The 3D bar rotates around its short *z*-axis (*x*: long axis and *y*: intermediate). The Hamiltonian that describes the motion for this model is:

$$H = \frac{1}{2}(p_x^2 + p_y^2 + p_z^2) + V(x,y,z,t) - \Omega_b(xp_y - yp_x) \equiv Energy$$

This model consists of the superposition of potentials describing an axisymmetric part and a bar component of the galaxy (Manos, Bountis, Ch.S., 2013, J. Phys. A).

a) Axisymmetric component:

$$M_S + M_B(t) + M_D(t) = 1, \quad \text{with} \quad M_B(t) = M_B(0) + \alpha t$$

i) Plummer sphere:

$$V_{sphere}(x,y,z) = -\frac{GM_S}{\sqrt{x^2 + y^2 + z^2 + \varepsilon_s^2}}$$

ii) Miyamoto–Nagai disc:

$$V_{disc}(x,y,z) = -\frac{GM_D(t)}{\sqrt{x^2 + y^2 + (A + \sqrt{B^2 + z^2})^2}}$$

b) Bar component:

$$V_{bar}(x,y,z) = -\pi Gabc \frac{\rho_c}{n+1} \int_\lambda^\infty \frac{du}{\Delta(u)} (1 - m^2(u))^{n+1},$$

(Ferrers bar)

$$\rho_c = \frac{105}{32\pi} \frac{GM_B(t)}{abc}$$

$$\text{where } m^2(u) = \frac{x^2}{a^2+u} + \frac{y^2}{b^2+u} + \frac{z^2}{c^2+u}, \quad \Delta^2(u) = (a^2+u)(b^2+u)(c^2+u),$$

n: positive integer ($n = 2$ for our model) , λ: the unique positive solution of $m^2(\lambda) = 1$

Its density is:

$$\rho = \begin{cases} \rho_c (1 - m^2)^n, & \text{for } m \le 1 \\ 0, & \text{for } m > 1 \end{cases}, \quad \text{where } m^2 = \frac{x^2}{a^2} + \frac{y^2}{b^2} + \frac{z^2}{c^2}, \quad a > b > c \text{ and } n = 2.$$

Time-dependent 2D barred galaxy model

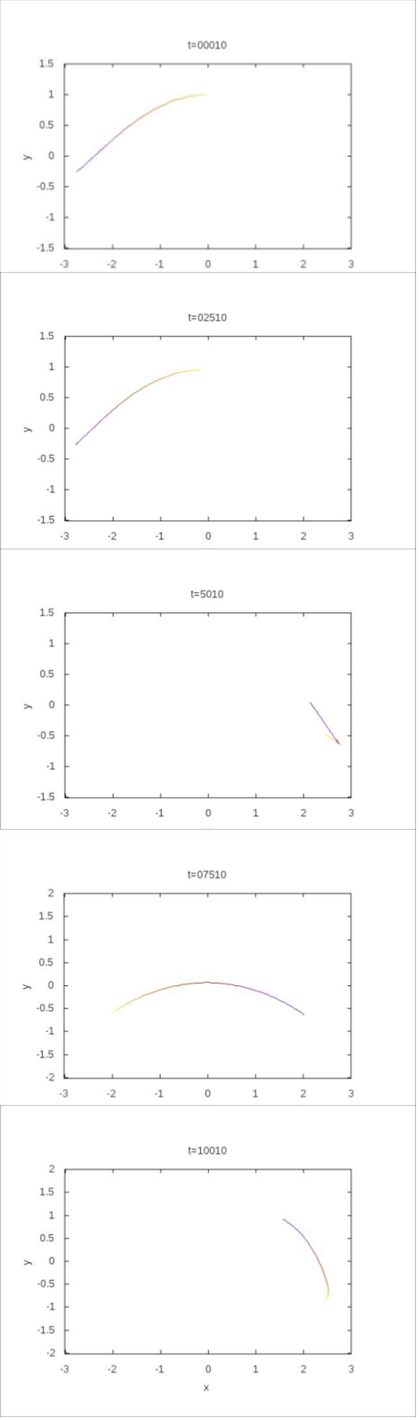

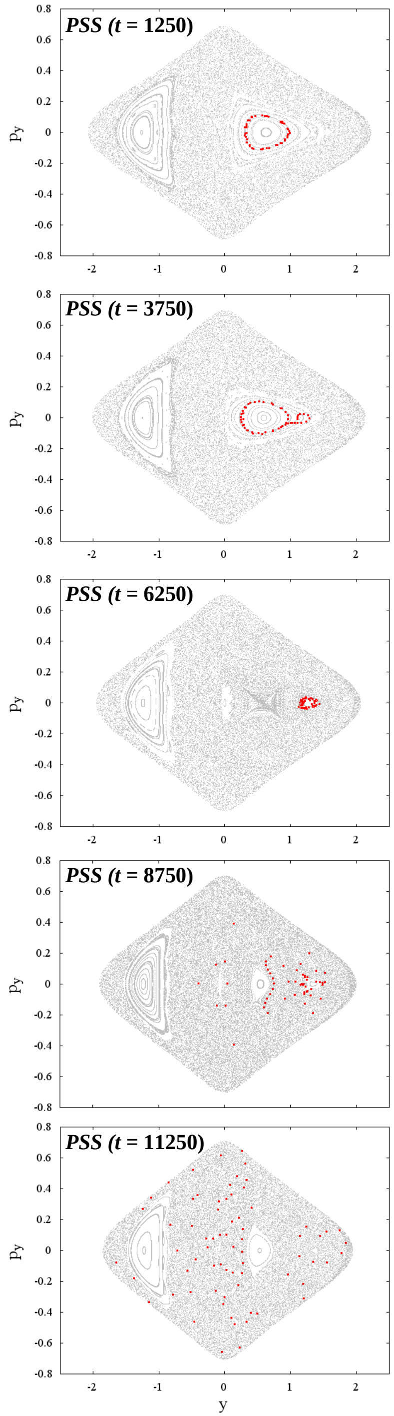

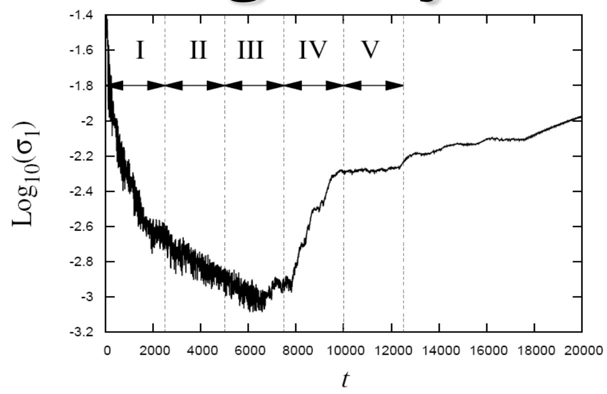

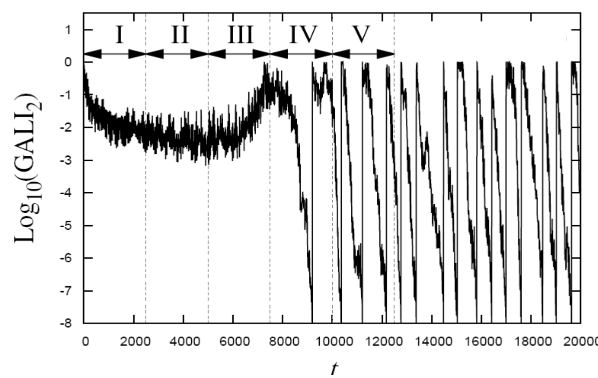

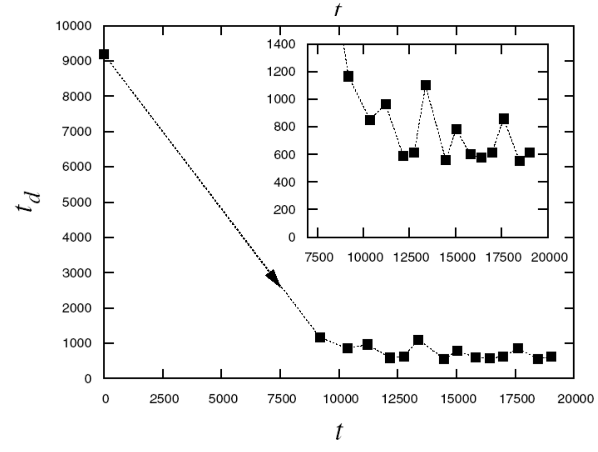

Time-dependent 3D barred galaxy model

Interplay between chaotic and regular motion

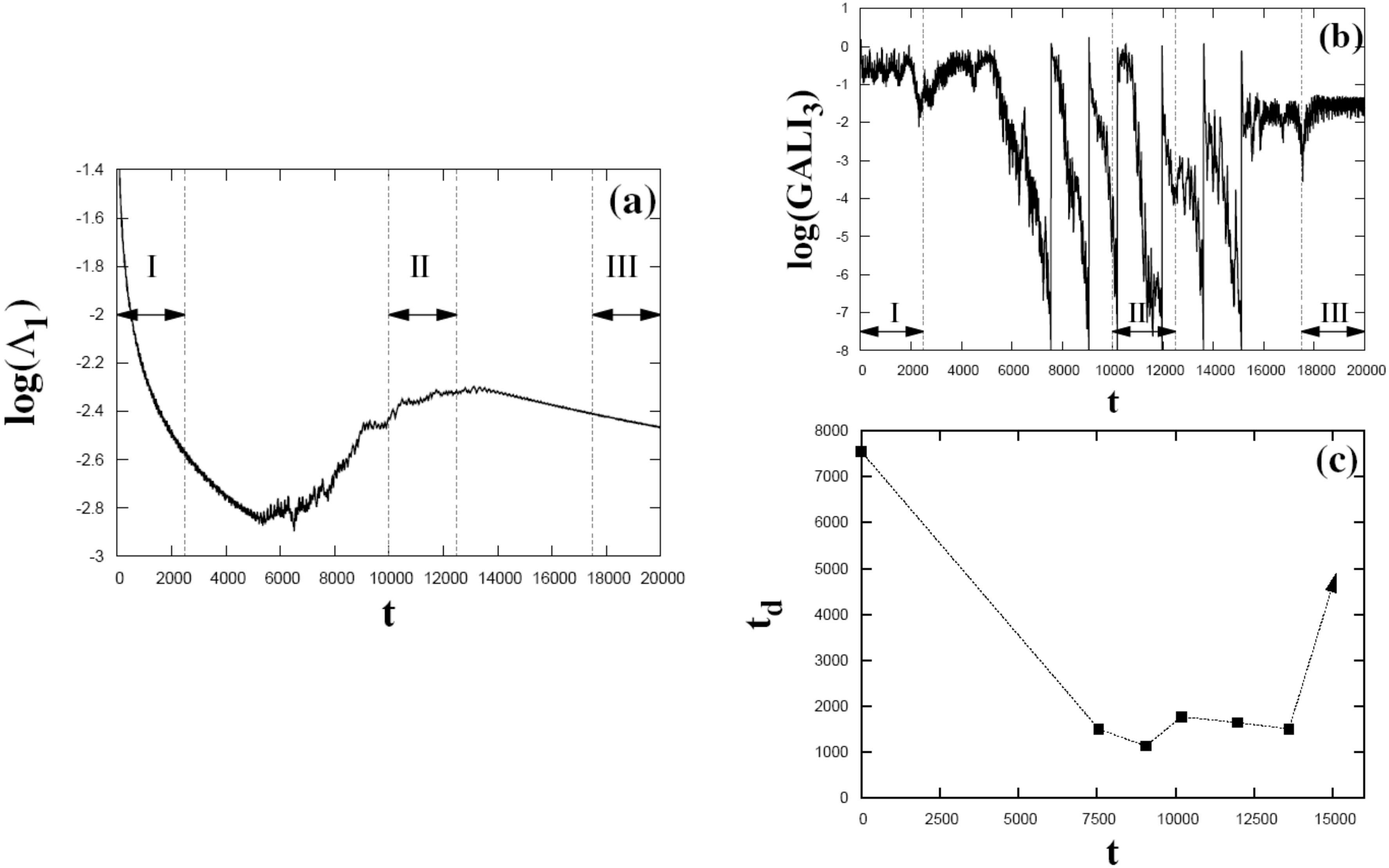

Summary

- **We discussed methods of chaos detection based on**
  - ✓ **the visualization of orbits**
  - ✓ **the numerical analysis of orbits**
  - ✓ **the evolution of deviation vectors (variational equations – tangent map)**

Summary

- **We discussed methods of chaos detection based on**
  - ✓ **the visualization of orbits**
  - ✓ **the numerical analysis of orbits**
  - ✓ **the evolution of deviation vectors (variational equations – tangent map)**
- **The Smaller (SALI) and the Generalized (GALI) ALignment Index methods are fast, efficient and easy to compute chaos indicator.**
- **Behaviour of the Generalized ALignment Index of order k ($GALI_k$):**
  - ✓ **Chaotic motion: it tends exponentially to zero**
  - ✓ **Regular motion: it fluctuates around non-zero values (or goes to zero following power-laws)**

Summary

- **We discussed methods of chaos detection based on**
  - ✓ **the visualization of orbits**
  - ✓ **the numerical analysis of orbits**
  - ✓ **the evolution of deviation vectors (variational equations – tangent map)**
- **The Smaller (SALI) and the Generalized (GALI) ALignment Index methods are fast, efficient and easy to compute chaos indicator.**
- **Behaviour of the Generalized ALignment Index of order k ($GALI_k$):**
  - ✓ **Chaotic motion: it tends exponentially to zero**
  - ✓ **Regular motion: it fluctuates around non-zero values (or goes to zero following power-laws)**
- **$GALI_k$ indices :**
  - ✓ **can distinguish rapidly and with certainty between regular and chaotic motion**
  - ✓ **can be used to characterize individual orbits as well as "chart" chaotic and regular domains in phase space**
  - ✓ **can identify regular motion on low–dimensional tori**
  - ✓ **are perfectly suited for studying the global dynamics of multidimentonal systems, as well as of time-dependent models**

Main References I

- **The color and rotation (CR) method**
  - ✓ Patsis P. A. & Zachilas L (1994) Int. J. Bif. Chaos, 4, 1399
  - ✓ Katsanikas M & Patsis P A (2011) Int. J. Bif. Chaos, 21, 467
  - ✓ Katsanikas M, Patsis P A & Contopoulos G. (2011) Int. J. Bif. Chaos, 21, 2321

- **The 3D phase space slices (3PSS) technique**
  - ✓ Richter M, Lange S, Backer A & Ketzmerick R (2014), Phys. Rev. E 89, 022902
  - ✓ Lange S, Richter M, Onken F, Backer A & Ketzmerick R (2014), Chaos 24, 024409
  - ✓ Onken F, Lange S, Ketzmerick R & Backer A (2016), Chaos 26, 063124

- **Frequency Analysis**
  - ✓ Laskar J (1990) Icarus, 88, 266
  - ✓ Laskar J, Froeschle C &Celletti A (1992) Physica D, 56, 253
  - ✓ Laskar J (1993) Physica D, 67, 257
  - ✓ Bartolini R, Bazzani A, Giovannozzi M, Scandale W & Todesco E (1996) Part. Accel. 52, 147
  - ✓ Laskar J (1999) in Hamiltonian systems with three or more degrees of freedom (ed. Simo C / Plenum Press) p 134

- **Lyapunov exponents**
  - ✓ Oseledec V I (1968) Trans. Moscow Math. Soc., 19, 197
  - ✓ Benettin G, Galgani L, Giorgilli A &Strelcyn J-M (1980) Meccanica, March, 9
  - ✓ Benettin G, Galgani L, Giorgilli A &Strelcyn J-M (1980) Meccanica, March, 21
  - ✓ Wolf A, Swift J B, Swinney H L &Vastano J A (1985) Physica D, 16, 285
  - ✓ Ch.S. (2010) Lect. Notes Phys., 790, 63

Main References II

- **0-1 test**
  - ✓ Gottwald G A & Melbourne I (2004) Proc. R. Soc. A, 460, 603
  - ✓ Gottwald G A & Melbourne I (2005) Physica D, 212, 100
  - ✓ Gottwald G A & Melbourne I (2009) SIAM J. Appl. Dyn., 8, 129
  - ✓ Gottwald G A & Melbourne I (2016) Lect. Notes Phys., 915, 221

- **FLI – OFLI – OFLI2**
  - ✓ Froeschle C, Lega E & Gonczi R (1997) Celest. Mech. Dyn. Astron., 67, 41
  - ✓ Guzzo M, Lega E & Froeschle C (2002) Physica D, 163, 1
  - ✓ Fouchard M, Lega E, Froeschle C & Froeschle C (2002) Celest. Mech. Dyn. Astron., 83, 205
  - ✓ Barrio R (2005) Chaos Sol. Fract., 25, 71
  - ✓ Barrio R (2006) Int. J. Bif. Chaos, 16, 2777
  - ✓ Lega E, Guzzo M & Froeschle C (2016) Lect. Notes Phys., 915, 35
  - ✓ Barrio R (2016) Lect. Notes Phys., 915, 55

- **MEGNO**
  - ✓ Cincotta P M & Simo (2000) Astron. Astroph. Suppl. Ser., 147, 205
  - ✓ Cincotta P M, Giordano C M & Simo C (2003) Physica D, 182, 151
  - ✓ Cincotta P M, & Giordano C M (2016) Lect. Notes Phys., 915, 93

- **RLI**
  - ✓ Sandor Zs, Erdi B & Efthymiopoulos C (2000) Celest. Mech. Dyn. Astron., 78, 113
  - ✓ Sandor Zs, Erdi B, Szell A & Funk B (2004) Celest. Mech. Dyn. Astron., 90 127
  - ✓ Sandor Zs & Maffione N (2016) Lect. Notes Phys., 915, 183

Main References III

- **SALI**
  - ✓ Ch.S. (2001) J. Phys. A, 34, 10029
  - ✓ Ch.S., Antonopoulos Ch, Bountis T C & Vrahatis M N (2003) Prog. Theor. Phys. Supp., 150, 439
  - ✓ Ch.S., Antonopoulos Ch, Bountis T C & Vrahatis M N (2004) J. Phys. A, 37, 6269
  - ✓ Bountis T & Ch.S. (2006) Nucl. Inst Meth. Phys Res. A, 561, 173
  - ✓ Boreaux J, Carletti T, Ch.S. &Vittot M (2012) Com. Nonlin. Sci. Num. Sim., 17, 1725
  - ✓ Boreaux J, Carletti T, Ch.S., Papaphilippou Y & Vittot M (2012) Int. J. Bif. Chaos, 22, 1250219

- **GALI**
  - ✓ Ch.S., Bountis T C & Antonopoulos Ch (2007) Physica D, 231, 30
  - ✓ Ch.S., Bountis T C & Antonopoulos Ch (2008) Eur. Phys. J. Sp. Top., 165, 5
  - ✓ Gerlach E, Eggl S & Ch.S. (2012) Int. J. Bif. Chaos, 22, 1250216
  - ✓ Manos T, Ch.S. & Antonopoulos Ch (2012) Int. J. Bif. Chaos, 22, 1250218
  - ✓ Manos T, Bountis T & Ch.S. (2013) J. Phys. A, 46, 254017

- **Reviews on SALI and GALI**
  - ✓ Bountis T C & Ch.S. (2012) 'Complex Hamiltonian Dynamics', Chapter 5, Springer Series in Synergetics
  - ✓ Ch.S. & Manos T (2016) Lect. Notes Phys., 915, 129

A …shameless promotion

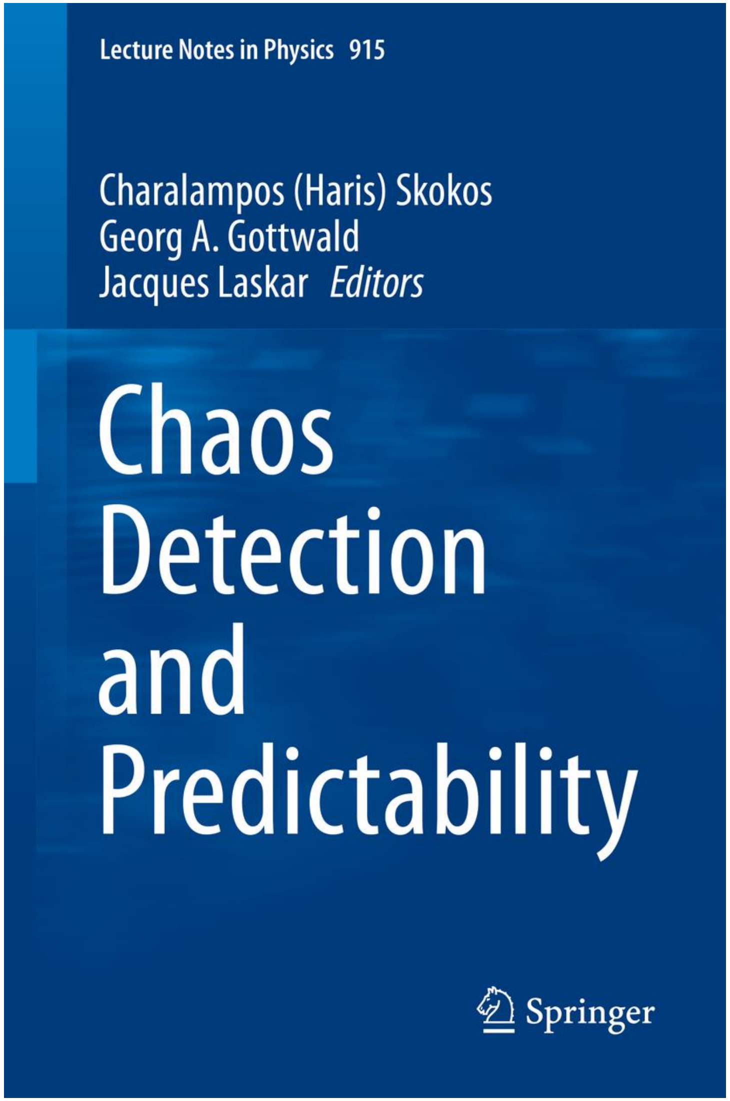

2016, Lect. Notes Phys., 915, Springer

Contents

1. **Parlitz:** Estimating Lyapunov Exponents from Time Series
2. **Lega, Guzzo, Froeschlé:** Theory and Applications of the Fast Lyapunov Indicator (FLI) Method
3. **Barrio:** Theory and Applications of the Orthogonal Fast Lyapunov Indicator (OFLI and OFLI2) Methods
4. **Cincotta, Giordano:** Theory and Applications of the Mean Exponential Growth Factor of Nearby Orbits (MEGNO) Method
5. **Ch.S., Manos: The Smaller (SALI) and the Generalized (GALI) Alignment Indices: Efficient Methods of Chaos Detection**
6. **Sándor, Maffione:** The Relative Lyapunov Indicators: Theory and Application to Dynamical Astronomy
7. **Gottwald, Melbourne:** The 0-1 Test for Chaos: A Review
8. **Siegert, Kantz:** Prediction of Complex Dynamics: Who Cares About Chaos?